Catarina Isabel Coelho Vargas

Salinity patterns adjustment to climate change in Ria de Aveiro

Ajustamento dos padrões salinos a mudanças climáticas na Ria de Aveiro

Universidade de Aveiro Departamento de Física
2012

Catarina Isabel Coelho Vargas

Salinity patterns adjustment to climate change in Ria de Aveiro

Ajustamento dos padrões salinos a mudanças climáticas na Ria de Aveiro

Dissertação apresentada à Universidade de Aveiro para cumprimento dos requisitos necessários à obtenção do grau de Mestre em Ciências do Mar e das Zonas Costeiras, realizada sob a orientação científica do Prof. Doutor João Miguel Sequeira Silva Dias, Professor Auxiliar do Departamento de Física da Universidade de Aveiro e co-orientação do Doutor Nuno Alexandre Firmino Vaz, Investigador Auxiliar no Centro de Estudos do Ambiente e do Mar (CESAM) da Universidade de Aveiro.

o júri

Presidente   Prof.ª Doutora Filomena Maria Cardoso Pedrosa Ferreira Martins
                          Professora Associada do Departamento de Ambiente e Ordenamento da Universidade de Aveiro

Arguente   Doutor João Daniel Alonso Antão Lencart e Silva
                          Investigador auxiliar do CESAM e Departamento de Física da Universidade de Aveiro

Orientador   Prof. Doutor João Miguel Sequeira Silva Dias
                          Professor auxiliar do Departamento de Física da Universidade de Aveiro

Co-orientador   Doutor Nuno Alexandre Firmino Vaz
                          Investigador auxiliar do CESAM e Departamento de Física da Universidade de Aveiro

acknowledgements

This study was only possible thanks to the help, support and active collaboration of many people.

To my supervisors, Prof. Doutor João Miguel Dias and Doutor Nuno Alexandre Firmino Vaz, for the scientific supervision, shared knowledge, patience, trust and advice.

To my friends and colleagues at NMEC working group, for their availability, support and encouragement, especially during the last months.

To my great friends, for their presence even though some only from the distance.

To my family, always present in all circumstances, an anchor and sometimes exceeding themselves in their willing to help.

To the "new family" in Aveiro for their company, help and encouragement in every moment!

To Adriano, by the unconditional support in these last months.

keywords

Coastal lagoon; numerical modeling; salinity; climate change; sea level rise; river flow

abstract

Ria de Aveiro lagoon is a complex shallow water system located in the northern coast of Portugal. The interaction between tides and river flow, in particular the significant freshwater contribution from Vouga river for most of an average year, induces longitudinal salinity gradients, justifying Ria de Aveiro classification as a typically estuarine environment.

The adjustment of saline patterns induced by climate change may have consequences in the ecological equilibrium of this environment. Saline intrusion due to SLR and river flow decrease may induct saline stress in the fertile low-lying lands of Baixo Vouga and saline intrusion in aquifers.

In this context, this study intends to answer to the question: How do seasonal saline distribution patterns are expected to adjust to climate change in Ria de Aveiro lagoon? Only recently the scientific community began to explore this issue through numerical modeling studies applied to estuarine environments worldwide.

The MOHID 2D numerical model was used to simulate reference and future scenarios. The numerical grid used was updated with 2012 data and includes low lying adjacent lands, so that marginal flooding could be simulated. The hydrodynamic and the salt and heat transport models were calibrated with the RMS errors and Skill values reflecting the good performance of the model in reproducing salt transport processes.

As main contributors to water salinity patterns adjustment in an estuarine environment, mean sea level and river flow from main tributaries at wet and dry conditions were adopted as variables of this study. Thus, three Future scenarios for wet (A) and dry (B) conditions were defined: A1 and B1 to evaluate the isolated effect of local SLR projected; A2 and B2 considering the projected changes at daily average river flow of the main tributaries; and A3 and B3 combining SLR and river flow changes projected, therefore, the more realistic ones. Projections for the end of XXI century are based on A2 SRES scenario.

It can be concluded that in wet season projected scenarios the increase in saline concentration is more significant than for the dry season ones, being that increase more significant in the lagoon upstream regions. However, in dry season future scenarios the saline intrusion tends to go further inland due to the negligible freshwater inflow projected.

The results obtained, in particular: the salinity concentration increase and the salt inland intrusion; the upstream saline increase as consequence of river flow projected reduction; and the larger salinity increase in upper lagoon regions, are in accordance with the ones achieved in the majority of the studies related to SLR impact in estuaries salinity, found in literature.

This study could be expanded to other estuarine environments and other variables with influence in ecology of these environments.

palavras-chave

Laguna costeira; modelação numérica; salinidade; alterações climáticas; elevação do Nível Médio do Mar; escoamento fluvial

resumo

A Ria de Aveiro é um complexo sistema estuarino de águas pouco profundas localizado na costa norte de Portugal. A interação entre maré escoamento fluvial, em particular a importante contribuição do Rio Vouga ao longo de um ano médio, induz gradientes longitudinais de salinidade, justificando a classificação da Ria de Aveiro como ambiente tipicamente estuarino.

O ajustamento dos padrões salinos induzida por alterações climáticas pode ter consequências no equilíbrio ecológico deste ambiente. A intrusão salina devida à subida do Nível Médio do Mar (NMM) e a redução do escoamento fluvial poderá provocar *stress* salino nos terrenos férteis do Baixo Vouga e intrusão salina nos aquíferos.

Neste contexto, este estudo pretende responder à questão: Como é expectável que os padrões de distribuição salina se ajustem às alterações climáticas projetadas para a Ria de Aveiro? Só recentemente a comunidade científica começou a explorar esta temática através de estudos de modelação numérica aplicados a ambientes estuarinos espalhados pelo mundo.

Utilizou-se o modelo numérico MOHID 2D na simulação de cenários de referência e futuros. A malha numérica utilizada foi atualizada com dados de 2012 e inclui zonas baixas adjacentes para que a inundação marginal possa ser simulada. Os modelos hidrodinâmico e de transporte de sal e calor foram calibrados, tendo-se verificado valores de RMS e Skill reveladores da boa performance do modelo na reprodução dos processos de transporte de sal.

O NMM e o escoamento fluvial em estação húmida e seca foram adotados como variáveis neste estudo, por serem determinantes no ajustamento dos padrões de salinidade da água num ambiente estuarino. Foram definidos três cenários futuros para condições húmida (A) e seca (B): A1 e B1 para avaliar o efeito isolado da subida projetada do NMM; A2 e B2 considerando as alterações projetadas para o escoamento fluvial médio diário dos principais afluentes; e A3 e B3 combinando a subida do NMM e as alterações projetadas no escoamento fluvial, por conseguinte, mais realistas. As projeções para o final do séc. XXI têm por base o cenário A2 do SRES.

Conclui-se que o aumento da concentração salina é mais significativo nos cenários projetados para estação húmida que para os cenários futuros em estação seca, sendo esse aumento mais expressivo nas regiões montante dos canais. No entanto, nos cenários futuros para estação seca a intrusão salina tende a chegar a regiões mais interiores devido aos caudais negligenciáveis projetados. Os resultados obtidos, em particular: o aumento da concentração salina e a intrusão salina; o aumento da salinidade nas regiões mais interiores da laguna em consequência da redução projetada no escoamento fluvial; e o maior aumento da salinidade verificado nas regiões mais interiores, estão em acordo com os resultados obtidos na maioria dos estudos encontrados na literatura, abordando o impacte da subida do NMM na salinidade de estuários.

Este estudo poderá ser alargado a outros ambientes estuarinos e a outras variáveis com influência na ecologia destes ambientes.

Contents

List of Figures

List of Tables

_____

1 Introduction

1.1 Motivation and aims

Coastal lagoons are highly productive ecosystems in the transition between land and sea. Separated or partially isolated from the adjacent ocean by a sandy barrier (Kjerfve, 1986), they consist of saline shallow water bodies. These environments have a key role, from the biodiversity and habitats point of view, in providing valuable resources for the human activities, thus justifying the human concentration in these areas. They also constitute support for several economic activities such as fisheries, tourism, harbor facilities, aquaculture and research, among others (Alves *et al.*, 2011).

According to the 4th Intergovernmental Panel on Climate Change (IPCC) Report, it is expected an increase of coastal zones vulnerability in the 21st century mainly due to mean sea level (MSL) rise (Nicholls *et al.*, 2007). Flooding of low-lying lands, coastal erosion and salt water inland intrusion are key concerns due to MSL rise.

Scientific community has emphasized the study of coastal zones vulnerability to inundation and erosion phenomena due to MSL rise (Sánchez-Arcilla *et al.*, 2008; Nicholls *et al.*, 1999), and less attention has been given to the comprehension of salt intrusion increase in climate change scenarios, and their consequences to water quality and ecology in transition water bodies, and to the availability freshwater resources. Note that one of the requirements of the Water Framework Directive (2000/60/EC) and recently, of the Directive on the protection of groundwater against pollution and deterioration (2006/118/EC) is to avoid saline intrusion in groundwater bodies.

Effects of climate change in the salinity of these water bodies, as a consequence of MSL rise projected and changes in river inflows from main tributaries, should be evaluated in order to establish and implement effective adaptation and mitigation measures.

The study of salt dynamics in coastal lagoons induced by climate change impacts is still recent within the scientific community, although of fundamental importance given the negative consequences that may arise to these ecosystems, human activities and freshwater availability. Chapter 2 gives a detailed description of the scientific advances in this topic.

Hence, the main objective of this work is to respond to the fundamental question: How do seasonal saline distribution patterns are expected to adjust to climate change in a specific and complex coastal lagoon environment - Ria de Aveiro lagoon?

Ria de Aveiro is the most extensive coastal lagoon in Portugal with an adjacent surface of about 250 km^2 (Dias, 2001). This shallow mesotidal temperate lagoon is located in the northwestern Portuguese coast, and is the most dynamic in terms of physical and biogeochemical processes in Portugal (Vaz and Dias, 2008). It has a very irregular geometry, being characterized by narrow channels and by extensive intertidal areas, namely mud flats and salt marshes. In a coastal system like Ria de Aveiro, the salinity is mainly influenced by tides and freshwater from terrestrial drainage (Vaz, 2007).

Saline intrusion is one of the problems that most affect the surrounding populations of Ria de Aveiro. Saline stress is occurring in the fertile low-lying lands of Baixo Vouga. Once flooded by sea water, previously fertile lands are unsuitable for growing crops for several years because of the saline deposits which remain after the floods have receded (Frazão *et al.*, 2010).

The adjustment of the Ria de Aveiro water salinity patterns to changes in main forcing, induced by climate change, is investigated in this study through numerical modeling. This work intends also to obtain new zonations of the Ria de Aveiro physical limits for the end of the XXI century, applying the Venice System to the projected modeled results. After an exhaustive literature review, no studies were found of Venice System application as a tool to evaluate estuarine physical zonation adjustments resulting from projected climate change impact. So, this last objective constitutes a completely new application of the Venice System.

In this study, the MSL rise and changes in river flow regimes of the lagoon's main tributaries projected for the end of the XXI century according to A2 scenario defined in the Special Report on Emissions Scenarios (SRES) (Nakićenović and Swart, 2000) were considered. River flow regimes representative of wet and dry seasons were also taken into account.

1.2 Work structure

This work is divided into eight chapters. Chapter 1 describes the motivations and aims. The state of the art concerning expected impacts of climate change in coastal lagoons, modeling of salt adjustments and the Venice System are presented in Chapter 2. In Chapter 3 a global view of the study area, emphasizing salinity patterns is presented. Chapter 4 concerns the methodology followed in this work. Here, the numerical model (MOHID, www.mohid.com) applied is briefly described and presented the present and future scenarios designed to the accomplishment of this study goals. Chapter 5 includes the steps followed to obtain an actualized numerical grid including low-lying areas susceptible to flooding. The calibration of the hydrodynamic, and the salt and heat transport models calibration is also presented in this section.

In Chapter 6 the modeled results of potential climate change effects are presented. The maximum salinity changes along the main lagoon channels and the adjustments of the salinity fields over the whole lagoon are analyzed. Finally, modeled reference and projected seasonal zonations (wet and dry seasons) are compared to evaluate the effect of the changes impounded in the redistribution of the physical zonations. Work conclusions and some recommendations for future work are summarized in Chapter 7.

2 Climate change and salinity in water lagoons: State of the art

There is a scientific consensus that the world is facing global warming as a consequence of anthropogenic greenhouse gas emissions (Solomon *et al.*, 2007). MSL rise is expected to intensify flooding as well as induce flood of low-lying coastal areas, erosion of sandy beaches and lagoon sand barriers, landward intrusion of salt water in estuaries and aquifers with consequent freshwater shortage, and gradual loss of natural ecosystems in these environments (Nicholls *et al.*, 2007; FitzGerald *et al.*, 2008; Nicholls, 2010). Beare and Heaney (2002) and Robarts *et al.* (2005) refer the potential increase of salinity in estuaries and upstream sections as a consequence of projected river flow decrease.

MSL rise will also lead to a larger tidal range, as shown by Walters (1992) for the Delaware Estuary, and Zhong *et al.* (2008) and Najjar *et al.* (2010) for the Chesapeake Bay. In Ria de Aveiro case study, Lopes *et al.* (2011) projected an increase in tidal prism for spring (28%) and neap tide (35%), at A2 SRES scenario.

It should be noted that changes in the geomorphologic configuration of the estuarine system under study, the Ria de Aveiro lagoon, may enhance the impact of MSL rise regarding its saline characteristics. Indeed, Dias *et al.* (2011a) showed by analytical and numerical modeling that the deepening of the mouth's channel, resulting mainly from dredging operations to allow the safe access of increasing size ships to the Aveiro commercial port, increased the tidal amplitude across the lagoon between 1987/88 and 2002/03. The most significant changes in tidal amplitude occurred in headwater of the channels, representing a consequent increase in saline intrusion. During this period, the amplitude of the principal lunar semidiurnal constituent (M_2) showed an increase tendency of 4.52 mm/year in the inlet (Dias *et al.*, 2011a).

The scientific community just recently has shown its interest in estuarine modeling studies focused on the distribution adjustment of salinity concentration, induced by climate change (Gibson and Najjar, 2000; Hilton *et al.*, 2008).

The first study on the impact of climate change on salinity concentration distribution in estuarine environments dates from 1979, applied to Delaware Estuary (Hull and Tortoriello, 1979). In 2000, Gibson and Najjar retook the theme, modeling the impacts in Chesapeak Bay salinity induced by streamflow changes due to climate change. In fact, Chesapeak Bay is a prototype to modeling studies on the responses of estuarine environments to MSL rise and flow change as a consequence of climate change in North America costal margin (Hilton *et al.*, 2008; Najjar *et al.*, 2010; Hong and Shen, 2012).

Despite its importance, the study of this theme is still taking its first steps. Modeling studies can be found sparsely. A few examples are the study of a climate change scenario impact in the salinity distribution of the Weser estuary (Germany) (Grabemann *et al.*, 2001), or the response of thermohaline characteristics of Mar Menor (Mediterranean Sea, Spain) to A2 SRES scenario (de Pascalis *et al.*, 2012), and the assessment of MSL rise impacts on Gorai river network (in the South West region of Bangladesh) salt concentration and intrusion (Bhuiyan and Dutta, 2012). Recent studies have started to consider the combination of projected changes in other variables than mean sea level, like meteorological conditions or oceanic salinity and water temperature (de Pascalis *et al.*, 2012; Hong and Shen, 2012).

The results of these studies tend to a common answer: the salt concentration will increase in estuarine environments and brackish water will extend landward as MSL rises (Grabemann *et al.*,

2001; Bhuiyan and Dutta, 2011; Chua *et al.*, 2011; Hong and Shen, 2012; Rice *et al.*, 2012). The results obtained by de Pascalis *et al.* (2012) constitute the only exception to salt concentration increase tendency. Table 2.1 summarizes the main results obtained by these authors.

In the James River, Rice *et al.* (2012) found that in climate change conditions in the middle-to-upper river the salinity increase is larger than the one found in its lower and upper parts. Seasonal variations are projected for salt intrusion. River runoff may play a key role in seasonal salinity distribution in estuarine environments, which may be disrupted by climate change (Miller and Russell, 1992). Hong and Shen (2012) showed for Chesapeake bay that in dry periods salt intrusion presents larger values while in wet periods these values are smaller. The impact of sea-level rise on the salt intrusion length increases as river runoff decreases, in coherence with the finding obtained by Chua *et al.* (2011) for San Francisco Bay. In what concerns river flow scenarios, Gibson and Najjar (2000) estimated that a change in annual Susquehanna River would result in a change in annual mean salinity of opposite sign. Similarly, Najjar *et al.* (2010) expect a decrease in mean salinity during winter in Susquehanna River due to the projected flow increase during this season.

Salinity distribution, along a transitional water system, may determine its ecology, affecting the density and occurrence of species populations, occupying niches according to their salt tolerance (Attrill and Rundle, 2002). Variations in different time scales such as seasonal, fortnight or tidal cycle may induce the occurrence of longitudinal displacements of organism communities (Attril and Rundle, 2002).

The saline patterns perturbation of transitional waters, induced by climate change, has consequences in the ecological equilibrium of these highly productive natural environments (Nicholls *et al.*, 2007), forcing aquatic species populations to readapt, in terms of distribution and density, reason why it should be studied. The composition and diversity of biological communities can be disturbed, affecting species with commercial importance and increasing preservation costs (Eisenreich, 2005). For example, Rice *et al.* (2012) pointed out floral and faunal habitats at the Chesapeake Bay tributaries as being more susceptible to salinity increase due to MSL rise, especially the ones with limited tolerance ranges to salinity. Among fishery species, and according to Najjar *et al.* (2010), salinity distribution change will affect their distribution and abundance. Is predictable that "(…) a long-term salinity increase may irreversibly damage estuarine ecosystems" (Hilton *et al.*, 2008). Therefore, to better understand the ecology of an estuary it is fundamental to describe these systems in terms of saline gradients.

The Venice System (Anonymous, 1959) was created to study this issue, one of the most well-known salinity function zonation schemes. This scheme defines six fundamental sections provided with estuarine ecological identity. Table 2.2 summarizes the characteristics of each of the six sections.

The Venice System has gained wide application in describing the patterns of distribution among estuarine organisms (Burger *et al.*, 1993), and was, subsequently to its creation, expanded by Carriker (1967).

Table 2.1 Projected changes in saline distribution for different estuarine environments worldwide.

Case study	Climate change induced forcing, scenario(s) and model(s) used	Results	Publication
Chesapeake Bay, USA	- Different scenarios of river flow change - Autoregressive statistical models of monthly salinity variations	A change in annual Susquehanna River flow of 10% result in a change in annual mean salinity (of opposite sign) of about 1, 4, and 7% in the lower, middle, and upper mainstem Bay, respectively	Gibson and Najjar (2000)
Weser estuary, Germany	- MSL rise from 40 cm (low water) to 70 cm (high water) - Scenario based on the work of von Storch *et al.* (1998) - Numerical water quality and transport model (Müller *et al.* 1992)	Upstream boundary of the brackish-water zone is projected to be located on average 2 km further upstream	Grabemann *et al.* (2001)
Chesapeake Bay, USA	- MSL rise of 0.2 m - simple statistical model	Bay-averaged salinity increase of approximately 0.5	Hilton *et al.* (2008)
Gorai River network, Bangladesh	- MSL rise of 0.59 m - A2 SRES scenario - Salinity flux model integrated with an hydrodynamic model	Salinity increase by 0.9 at a distance of 80 km upstream of the river mouth	Bhuiyan and Dutta (2011)
San Francisco Bay, USA	- MSL rise - CCSM3-A2 global climate model - Hydrodynamic SUNTANS model	Salt water penetrates further into the Bay Salt concentration increase	Chua *et al.* (2011)
Mar Menor lagoon, Spain, Mediterranean Sea	- MSL rise - A2 SRES scenario - SHYFEM hydrodynamical model (Umgiesser and Bergamasco, 1995)	Decrease in mean salinity of 1.53	de Pascalis *et al.* (2012)
Chesapeake Bay, USA	- MSL rise of 1.0 m - Scenarios of U.S. Climate Change Science Program (CCSP, 2009) - Three-dimensional Hydrodynamic-Eutrophication Model (HEM-3D)	Salt intrusion length* will increase as much as 11 km during the low-flow period During the high-flow period, such increase is approximately 7 km	Hong and Shen (2012)
James River, a tributary of Chesapeake Bay, USA	- MSL rise of 1.0 m - Scenarios of U.S. Climate Change Science Program - Three-dimensional Hydrodynamic-Eutrophication Model (HEM-3D)	Salinity intrude about 10 km further upstream	Rice *et al.* (2012)

* Salt intrusion length defined as the distance from the estuarine environment mouth to the salt intrusion limit in the upper estuary where the bottom 0.5 isohaline is located.

Table 2.2 Venice System sections.

Designation	Estuarine environment location	Salinity concentration range
Limnetic zone	River	less than 0.5
Oligohaline zone	Top of the estuary	between 0.5 and 5
Mesohaline zone	Upper section of the estuary	between 5 and 18
Polihaline zone	Covering the middle and lower sections of the estuary	
	Middle section	between 18 and 25
	Lower section	between 25 and 30
Euhaline zone	Estuarine mouth	upper than 30

The description of an estuarine environment in terms of saline gradients and, therefore, of its ecological zonation, is even more relevant in a complex geomorfological system as Ria de

Aveiro (Dias *et al.*, 2001), which is strongly influenced by seasonal variations (Moreira *et al.*, 1993). The physical zonation based on Veneza System has already been applied to Ria de Aveiro by Dias *et al.* (2011a). The Ria de Aveiro zonation was obtained from salinity measurements conducted in four time periods representative of each season in mean tidal amplitude conditions, from October 2000 to July 2001. Main results of this study are presented at Section 3.2. However, remains unknown new seasonal future zonations resulting from climate change impacts in salinity distribution. This thesis aims to address this gap.

_____

3 Study area

3.1 General description

The Ria de Aveiro lagoon (Figure 3.1), located on the north-western Portuguese coast (40°38' N, 8°45' W), is the most extensive shallow mesotidal system in Portugal (Teixeira, 1994). Since its origin, the lagoon and sea connection migrated from Torreira to Mira, with the development of a sandy dune barrier bordering its west limit with the Atlantic Ocean. This dune barrier was interrupted in the beginning of 19th century (Abecasis, 1961), by the artificial opening of the present inlet (Barra de Aveiro) in the central area of the lagoon.
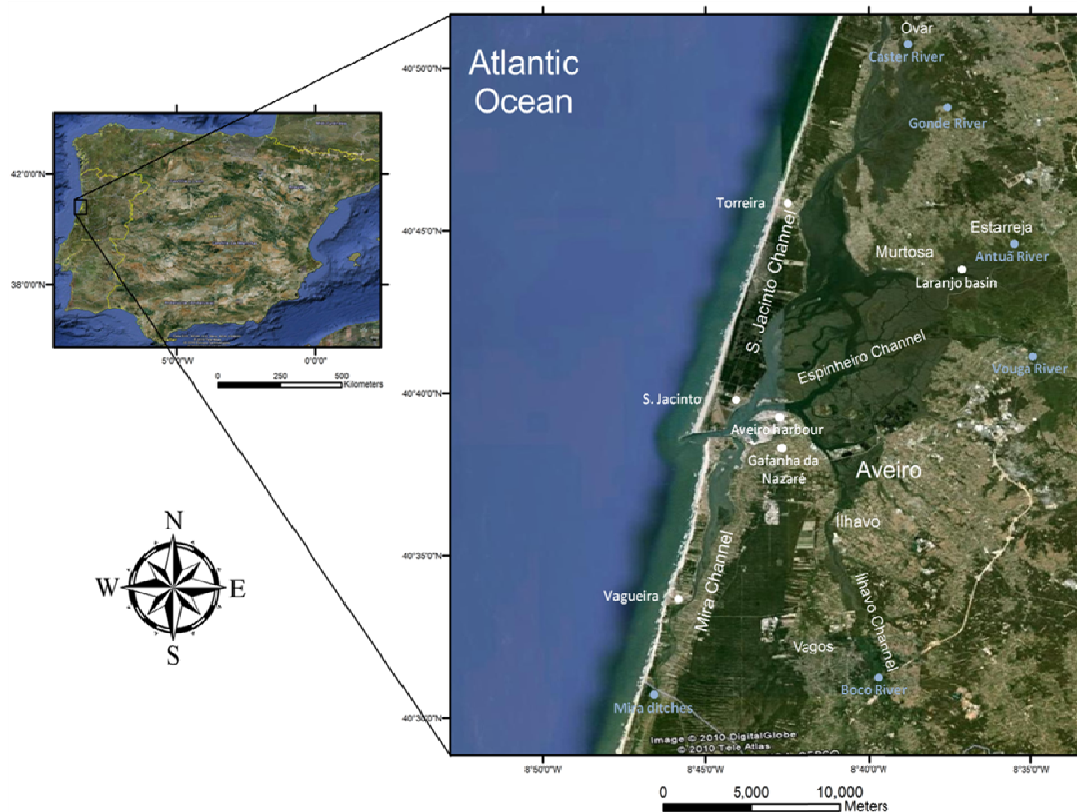
Adapted from: Mendes (2010)

Figure 3.1 Ria de Aveiro lagoon.

With a maximum width of 10 km and an extension parallel to the coast that reaches 45 km (Dias and Lopes, 2006), this lagoon presents an irregular geometry characterized by narrow channels and vast intertidal areas like mudflats, salt marches and saltpans. Four main branches spread from the mouth (see Figure 3.1): the Mira channel, an elongated shallow arm with 20 km length running southward; the S. Jacinto channel, extending for 29 km to the North; and the Ílhavo and Espinheiro channels, the shortest of the main channels with lengths of 15 km and 17 km, respectively (Dias, 2001).

Ria de Aveiro presents an average depth of 1 m relative to local datum. In navigation channels, near the mouth and commercial harbors depths can reach a depth of about 30 meters relative to local datum. The lagoon presents a significant variable area due to: the extensive intertidal areas; its small depth; and large tidal influence, reaching in spring tides a maximum area of 83 km^2 at high tide, reduced to a minimum of 66 km^2 at low tide (Dias, 2001).

Ria de Aveiro lagoon presents a typical estuarine behavior, denoting well defined saline longitudinal gradients between its mouth and the channels headwaters, as a consequence of important freshwater contributions from several tributaries during most of an average year. The importance of river inflow in the establishment of these saline gradients was shown by recent studies applied to Espinheiro channel (Figure 3.1), combining data measurements and modeling results analysis (Vaz *et al.*, 2005; Vaz and Dias, 2008).

Although several rivers discharge into Aveiro lagoon, the largest freshwater contribution in an average year comes from the Vouga river (an average flow of about 48 m^3/s), followed by Mira ditches (about 8m^3/s), Antuã river (about 3m^3/s) and Boco river (about 2m^3/s). These average river flows were calculated in the scope of this study, from estimates (period 1971-2000) obtained with the SWAT model (Neitsch *et al.*, 2011) by IST/MARETEC team for the DyEPlume Project (PTDC/MAR/107939/2008). The Vouga river discharges at the head of the Espinheiro channel's head and Antuã river joins the lagoon in the Laranjo basin, both discharging in the very complex central area of the lagoon. Mira ditches contribute with freshwater to the lagoon in its southwest limit, at the head of the Mira channel, while Boco river discharges in the lagoon's Southeast limit, in the Ílhavo channel's head. Caster and Gonde are rivers with a smaller contribution, discharging in the lagoon's northern channels. These tributaries discharge location is marked in Figure 3.1. A more detailed description about the freshwater contribution of the lagoon's main tributaries is presented in Sub-section 4.2.2.

The lagoon presents tidal amplitudes at the inlet of 0.6 m in neap tides and 3.2 m in spring tides, corresponding to a maximum and a minimum water level of 3.5 m and 0.3 m, respectively. The mean tidal range is about 2.0 m (Dias *et al.*, 2000). At the lagoon's mouth the tides are predominantly semidiurnal, with M_2 and S_2 constituents representing 88% and 10% of total tidal energy, respectively (Dias *et al.*, 2000; Dias, 2001).

Estimates of tidal prism at the lagoon's mouth range at maximum spring tide between 90×10^6 m^3 and 137×10^6 m^3, and at minimum neap tide between 31×10^6 m^3 and 35×10^6 m^3, depending on the tidal conditions and model used (lower estimates at spring and neap tides by Picado *et al.*, 2010, and higher estimates by Dias, 2001). The total estimated freshwater input, of about 1.8×10^6 m^3 during a tidal cycle (Moreira *et al.*, 1993), is very small when compared with this tidal prism range.

The lagoon's area covers two of the major aquifer systems identified by Portuguese National Water Institute (INAG, I.P.) in the West Mesocenozoic Edge – Aveiro Quaternary and Cretaceous aquifer systems. Due to their geologic characteristics, both present medium to high vulnerability to pollution, which can result from saline intrusion, industrial and agricultural activities.

According to Rebelo and Pombo (2001), Ria de Aveiro is considered the most important lagoon in the Portuguese littoral and one of the four main wetlands in the country. Indeed, it plays an important ecological role, being classified as a special area of conservation under the EU directives on the conservation of wild birds (79/409/EEC) and habitats (92/43/CEE), also offering good conditions for agricultural development alongside its borders. This lagoon is also considered one of the most important Southern European LTER Estuary reference study sites (http://www.lterportugal.net/). In these environments several economic activities such as aquaculture, fishing and shellfish collecting, depend on the lagoon's water quality and productivity.

_____

3.2 Horizontal salt patterns

In systems like Ria de Aveiro, the distribution of salinity and of other hydrological properties are conditioned by the balance between the spring/neap tidal cycle and the river flow. Despite the lower fluvial contribution in this system, freshwater inflow is essential in the establishment of saline patterns (Vaz _et al._, 2005). Vouga and Antuã are the main contributors for the establishment of these patterns. River discharges at S. Jacinto channel's head present a low inflow contribution. The high freshwater fraction at Mira channel can't be neglected and may have origin in a diffuse contribution of fresh groundwater.

This estuarine system can be considered vertically homogeneous during most of the year, mainly at dry seasons. The exception occurs with strong freshwater flows, when the lagoon shows weakly stratification, with higher expression at the downstream limit of the Espinheiro channel (Dias _et al._, 1999; Vaz and Dias, 2008).

Ria de Aveiro presents typical estuarine salinity patterns (Dias _et al._, 2011a), denoting longitudinal saline gradients from the lagoon's mouth to its channels head, more clear in higher river runoff.

A field and modeling study of Espinheiro channel (Vaz and Dias, 2008; Vaz _et al._, 2012) showed that when the river flow is weak, tide dominates the channel's hydrodynamic. For high river flows, freshwater may extend its influence beyond the lagoon's mouth (Dias _et al._, 1999; Vaz and Dias, 2008). At neap tide conditions, river flow reveals a relative stronger effect in the salinity horizontal patterns (Vaz _et al._, 2005). Vaz _et al._ (2005) showed that saline fronts are generated, migrating between 7th km to 8th km and between 8th km to 9th km (about 1 km difference) relative to the lagoon inlet, depending if the tide is a neap or a spring one, respectively. A saline front occurs when the salty water mixes with the incoming freshwater leading to a pronounced horizontal gradient of salinity. "This strong horizontal gradient seems to mark the boundary between two distinguished sectors: a marine estuary, in close connection with the sea, and an upper fluvial estuary characterized by the freshwater from the river, but still subject to a semidiurnal tidal effect." (Vaz _et al._, 2005).

A seasonal variability of the salinity distribution in Ria de Aveiro was confirmed by Dias _et al._ (2011a) while analyzing data from synoptic measurement of physical and biochemical parameters along the lagoon's channels, between October 2000 and July 2001. Sampling was conducted approximately in half flood tide conditions, during tides of average amplitude.

Analyzing these data Dias _et al._ (2011a) concluded that is notorious the seasonal and spatial salinity variation in the lagoon. Lower salinity concentrations were found during winter and in the beginning of spring. Salinity values lower than 4 were found in the headwaters of the channels and in the range of 10-18 across the lagoon's central zone and at the mouth. The highest values were measured during the Spring and Summer months (dry season). In these periods, maximum values higher than 30 were found in the lagoon central zone, and minima of about 18 in Espinheiro and Ílhavo channel's heads and in the upward intermediate zone of Mira channel and Laranjo Basin. In short, during the dry seasons, the saline intrusion was significant in a large extent, reaching the upstream regions of the main channels. In the wet seasons, a saline intrusion retreat was registered, as well as a reduction of the average lagoon salinity.

Dias _et al._ (2011a), following the Fairbridge (1980) definition for estuary, identified for each period under study the location and extension of the three sectors: a) lower or marine estuary

(L/M) with a salinity higher than 25; b) middle estuary (M) with salinity between 18 and 25; and c) upper or fluvial estuary (U/F) with salinity lower than 18. In autumn the overall lagoon presents L/M characteristics, with exception to the Laranjo basin, Espinheiro channel's head and surroundings, Ílhavo channel's head and Mira channel's upper zone, where salinity values are typical of M. In winter, most of the channels can be classified as U/F, excepting the lagoon's mouth and Mira channel's lower zone with L/M or M characteristics. In spring, the entire lagoon presents U/F characteristics. In summer, almost all the lagoon presents L/M characteristics, with exception to Laranjo basin and surrounding zone, and Mira and Ílhavo channel's heads with salinity values typical of U/F. Intermediate zones exhibit salinity values typical of M.

The Venice System zonation (described at Chapter 2; Carriker, 1967) was applied to the salinity distribution at each measurement period. Table 3.1 summarizes these results, whose interpretation is best understood reading Dias *et al.* (2011a) article.

Table 3.1 Ria de Aveiro longitudinal zonations according to Venice System (Dias *et al.*, 2011b).

Longitudinal zones	Autumn 2000 (2/10 - 4/10)	Winter 2000 (29/11 and 14/12)	Spring 2001 (29/3 - 30/3, and 5/4)	Summer 2001 (26/6 – 27/6)
Limnetic	–––	Laranjo basin, and Espinheiro and Ílhavo channel's heads	Laranjo basin in a lower extension than observed in Winter, Espinheiro channel's head and surrounding zone, and Mira channel's head	–––
Oligohaline	–––	Mira channel's head, and about middle of the upstream extension of S. Jacinto, Espinheiro and Ílhavo channels	Upstream sections of the main channels	Mira channel's head
Mesohaline	Mira channel's head	Significant e tension of the four main channels	Downstream sections of the main channels, including lagoon's mouth	Ílhavo and Espinheiro channel's heads, Laranjo basin and surrounding zone, and middle section of Mira channel
Polihaline (middle section)	Laranjo basin, Espinheiro channel's head and surrounding zone, Ílhavo channel's head, and middle section of Mira channel	Inlet zone and lower estuary	–––	S. Jacinto channel's head and transitional zones in the three remaining channels
Polihaline (lower section)		Small section of Mira channel	–––	
Euhaline	Most of Ria de Aveiro and downstream limit of Mira channel	–––	–––	Lagoon's mouth and most of the lagoon central zone, with a larger extension upstream S. Jacinto channel

All section types were identified in Ria de Aveiro. Their existence, location and extension show a strong seasonal variability.

_____

4 Methodology

The salt distribution in Ria de Aveiro is modeled in this study using the MOHID hydrodynamic model, a numerical model under continuous development by MARETEC – Marine and Environmental Center group of the Instituto Superior Técnico (Santos, 1995; Martins *et al.*, 2001; Leitão, 2003; Leitão *et al.*, 2005). It has been applied with success to different coastal, estuarine and shallow water environments, showing its ability to model complex features of flows as found in Ria de Aveiro (Trancoso *et al.*, 2005; Vaz *et al.*, 2005, 2007a, 2007b, 2009; Vaz and Dias, 2011). MOHID model is described in the next Section, in what concerns governing equations and boundary conditions.

A previous numerical grid was actualized and improved as described in Section 5.1. The MOHID hydrodynamic module was calibrated and validated (Section 5.2) using two recent independent data sets of 2002/2003 and June 1997 respectively. These data sets consist of sea surface elevation and current velocity time series, with current velocity measurements being only included in the data set used for validation. The successful hydrodynamic calibration was followed by the salt and heat transport module calibration, confronting the model results with salt and heat data collected in the dry period of July 2006 (Section 5.3).

For the Aveiro region are projected a relative MSL rise (Sub-section 4.2.1) and a seasonal reduction of the fluvial flow regime (Sub-section 4.2.2). Several authors (Gibson and Najjar, 2000; Bhuiyan and Dutta, 2011; see Chapter 2) predict, for these conditions, a salinity increase in estuarine environments and a further upstream relocation of the brackish-water zone. In an actual average year, this situation occurs in dry conditions. Based on this, the good accuracy achieved when calibrating the salt model transport with data measured in dry conditions ensures the model ability to simulate future projected conditions with significant confidence.

Scenarios designed for different combinations of local MSL rise projected and river flow forcing at the end of XXI century (A2 SRES scenario) are presented and described in Section 4.2.

4.1 Numerical model description

The MOHID model is a 3D baroclinic model using a finite volumes approach (Chippada *et al.*, 1998) and adopting an Arakawa C staggered grid in the horizontal direction (Arakawa and Lamb, 1977) to perform the spatial discretization, the grid being defined explicitly. The temporal discretization is carried out using a semi-implicit algorithm: the ADI (Alternate Direction Implicit), described in Abbott and Basco (1994). In all simulations it was used the 6 equation algorithm discretization scheme by Leendertse (1967), more conveniently when modeling systems with intertidal areas. This algorithm calculates, alternatively, one component of horizontal velocity implicitly, while the other is calculated explicitly, avoiding the calculation of the internal and external modes with different time steps (Leitão, 2003). This model assumes the hydrostatic equilibrium, as well as the Boussinesq approximation.

Ria de Aveiro is a shallow coastal lagoon with a complex morphology, presenting well mixed characteristics (Dias *et al.*, 1999). Therefore, in this study MOHID was implemented in a 2D model.

4.1.1 The governing equations

MOHID solves the three-dimensional incompressible primitive equations. Hydrostatic equilibrium is assumed as well as the Boussinesq and Reynolds approximations. From the hydrostatic approximation is obtained:

$$p(z) = p_{atm} + \rho g(\eta - z) + g \int_z^\eta \eta \rho' \, dz \tag{4.1}$$

where p is pressure, p_{atm} is the atmospheric pressure, ρ is density, ρ' is its anomaly, g is gravity, η is the free surface and z the depth where pressure is calculated.

This equation relates pressure at any depth with the atmospheric pressure at the sea surface, the sea level and pressure anomaly integrated between that level and the surface. Using the Boussinesq approximation it is possible to describe the total pressure gradient as the sum of the gradients of the atmospheric pressure, the sea surface elevation (barotropic pressure gradient) and the density distribution (baroclinic pressure gradient):

$$\frac{\partial p}{\partial x_i} = \frac{\partial p_{atm}}{\partial x_i} - g\rho_0 \frac{\partial \eta}{\partial x_i} - g \int_z^\eta \eta \frac{\partial \rho'}{\partial x_i} dz \tag{4.2}$$

This decomposition is substituted in the 3D incompressible primitive equations and yields to the mass momentum equation:

$$\frac{\partial u_i}{\partial t} + \frac{\partial (u_i u_j)}{\partial x_j} = -\frac{1}{\rho_0} \frac{\partial p_{atm}}{\partial x_i} - g \frac{\rho(\eta)}{\rho_0} \frac{\partial \eta}{\partial x_i}$$

$$-\frac{g}{\rho_0} \int_{x_3}^\eta \frac{\rho'}{\partial x_i} dx_3 + \frac{\partial}{\partial x_j} \left(v \frac{\partial u_i}{\partial x_j} \right) - 2\varepsilon_{ijk}\Omega_j u_k \tag{4.3}$$

Equation (4.3) shows how the horizontal velocity components are calculated, where u_i are the velocity vector components in the Cartesian x_i directions, u_j are the velocity vector components in the Cartesian x_j directions and v is the turbulent viscosity. ρ_0 is the reference density, Ω is the Earth's rotation velocity and ε is the alternate tensor.

The mass balance equation (continuity) is represented by:

$$\frac{\partial u_i}{\partial x_i} = 0 \tag{4.4}$$

The free surface equation is obtained by integrating the continuity equation over the whole water column. The integration limits are the free surface elevation, η *(x, y)*, and the bottom, $-h$ (where h is the depth).

$$\frac{\partial \eta}{\partial t} = -\frac{\partial}{\partial x_1} \int_{-h}^\eta u_1 \, dx_3 - \frac{\partial}{\partial x_2} \int_{-h}^\eta u_2 \, dx_3 \tag{4.5}$$

The model solves a transport equation for water salinity, temperature or any other tracer. The formulation of the advection-diffusion solved by MOHID is:

$$\frac{\partial \alpha}{\partial t} + u_j \frac{\partial \alpha}{\partial x_j} = \frac{\partial \alpha}{\partial x_j} \left(K \frac{\partial \alpha}{\partial x_i} \right) + \text{FP} \tag{4.6}$$

where α is the transported property concentration (salinity), K is the diffusion coefficient and FP is a possible source or sink term.

The bottom shear stress $\vec{\tau}$ is imposed using the formulation proposed by Chézy (Dronkers, 1964), where $\vec{\tau}$ is proportional to the velocity squared (Equation 4.7) and the drag coeficiente C_D can be parameterized in terms of the Manning friction coefficient n (Equation 4.8):

$$\vec{\tau} = C_D|\vec{V}|V \tag{4.7}$$

$$C_D = gn^2H^{1/3} \tag{4.8}$$

where $\vec{V}$ is the horizontal velocity vector and H ($H = h + \eta$) is the depth of the water column.

4.1.2 Boundary Conditions

Several types of boundaries were used in this application: free surface, bottom, lateral closed boundary, lateral opened boundary and moving boundary.

At the ocean open boundary the free surface elevation is imposed and at the river boundaries the flow is specified. A free slip condition is imposed at the lateral boundary condition by specifying a zero normal component of mass and momentum diffusive fluxes at cell faces in contact with land. No mass fluxes at the surface and bottom were considered.

Moving boundaries are closed boundaries whose position varies with time. This situation appears in domains with large intertidal zones, like Ria de Aveiro. The uncovered cells must be tracked and with this purpose a criterion base in Figure 4.1 is used. *HMIN* is the depth bellow which cell is considered uncovered. In this case a thin volume of water above the uncovered cell is conserved. The cell of position *i, j* is considered when one of the two following situations is true (Leitão, 2003; Vaz *et al.*, 2005):
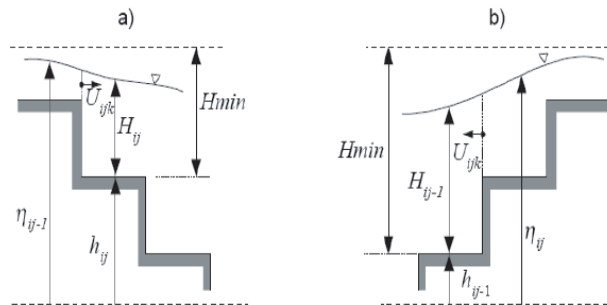
Figure 4.1 Conditions for a cell to be considered uncovered (moving boundaries) (Leitão, 2003).

$$H_{ij} < HMIN \wedge \eta_{ij-1} < -h_{ij} + HMIN \tag{4.9}$$
$$H_{ij-1} < HMIN \wedge \eta_{ij} < -h_{ij-1} + HMIN \tag{4.10}$$

The second condition of Equation (4.9) assures that the cell is not being covered by the tidal wave propagation from left to right and the second condition of Equation (4.10) assures that the cell is not being covered by the tidal wave propagation from right to left. The noise formed by the abrupt change in velocity at the dry cells is controlled with a careful choice of $HMIN$ (in this simulation: $HMIN$ = 0.15 m) (Leendertse and Liu, 1978).

4.2 Scenarios Design

In a system like Ria de Aveiro, the salinity spatial and temporal distribution is strongly dependent on the balance between the spring/neap tidal cycle and the river flow. Projected changes in mean sea level and river flow, in the scope of climate change scenarios, will certainly have implications in salinity distribution patterns. To study these implications, actual and future scenarios are defined based on realistic forcing combinations for dry and wet conditions. The salinity distribution patterns resulting from reference scenarios will allow assessing the impacts arising from changes in the forcing imposed in future scenarios. Local MSL rise and river flow projections are derived from A2 SRES scenario defined in the Special Report on Emissions Scenarios (SRES).

Dry and wet seasons are defined as the three consecutive months which present, respectively, the lowest and the highest average monthly mean flow (Figure 4.2). The average monthly mean flows estimated in this work were obtained from the daily flow series simulated with the SWAT model by IST/MARETEC team in the scope of DyEPlume Project (PTDC/MAR/107939/2008), for the period 1971-2000. For this estimative were chosen the simulations for the Vouga river as it is the main lagoon's tributary. Analyzing this figure, according to the above definition, dry season corresponds to July, August and September, while the wet season corresponds to January, February and March, wet season beginning three months after the dry season.
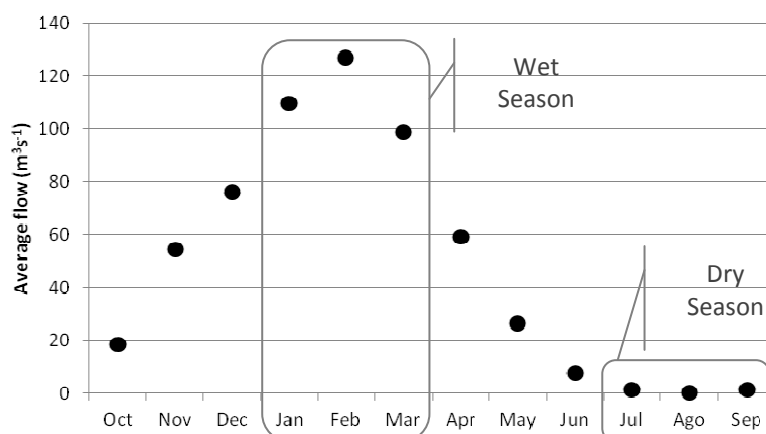
Figure 4.2 Vouga's averages of monthly mean flow obtained from estimated daily mean flow for the period 1971-2000.

As river flow and mean sea level constitute the forcing whose change impact in lagoon's salinity is intended to be studied, the remaining parameters/forcing are set by default in all the scenarios: salinity of 36.5 in the ocean open boundary and of 0 in the landward boundary. Atmospheric forcing is assumed to have a negligible effect in the simulation of salt transport. Indeed the heat transport is not considered in this study.

A mean sea level of 2.02 m referenced to chart datum was imposed at the ocean open boundary for future scenarios assuming a constant MSL and for reference scenarios. For all other future scenarios was imposed a MSL rise for the end of the century (2091-2100 relative to 1980-1999) of 0.42 m, as obtained by Lopes *et al.* (2011). The Lopes *et al.* (2011) MSL rise estimative procedure is briefly described in Sub-section 4.2.1.

_____

Landward boundaries were forced with average daily mean flow time series, for wet and dry conditions, estimated in this work from the SWAT simulations. As referred above, the SWAT model allowed IST/MARETEC team to estimate and project (A2 SRES scenario) daily mean flow time series for 1971-2000 and 2071-2100, respectively. The estimated average daily mean flow time series for wet and dry seasons are presented at Figure 4.4 in Sub-section 4.2.2 for the main Ria de Aveiro tributaries.

Two reference scenarios are defined (Figure 4.3): the A0 scenario imposing a reference sea level of 2.02 m and the average daily mean flow time series estimated for wet season at present conditions (time series presented in Figure 4.4); and the B0 scenario whose only difference to A0 scenario is the average daily mean flow time series considered, in this case estimated for dry season (Figure 4.4).

For the six projected scenarios defined (Figure 4.3), A1, A2 and A3 are referent to wet season, while B1, B2 and B3 correspond to dry season. At A1 and B1 scenarios is prescribed a relative MSL rise of 0.42 m, maintaining the river flow forcing of A0 and B0 scenarios, to evaluate the isolated effect of MSL rise. A2 and B2 diverge from A0 and B0 scenarios by imposing the average daily mean flow series projected for the end of the century (Figure 4.4), thus evaluating river flow change isolated impact. A3 and B3 scenarios correspond to the worst but more realistic conditions being studied, combining MSL rise and river flow projected for the end of the 21st century.

The reference and future average daily mean flow time series taken as forcing for all the defined scenarios were obtained in the scope of this study as described in Sub-section 4.2.2.
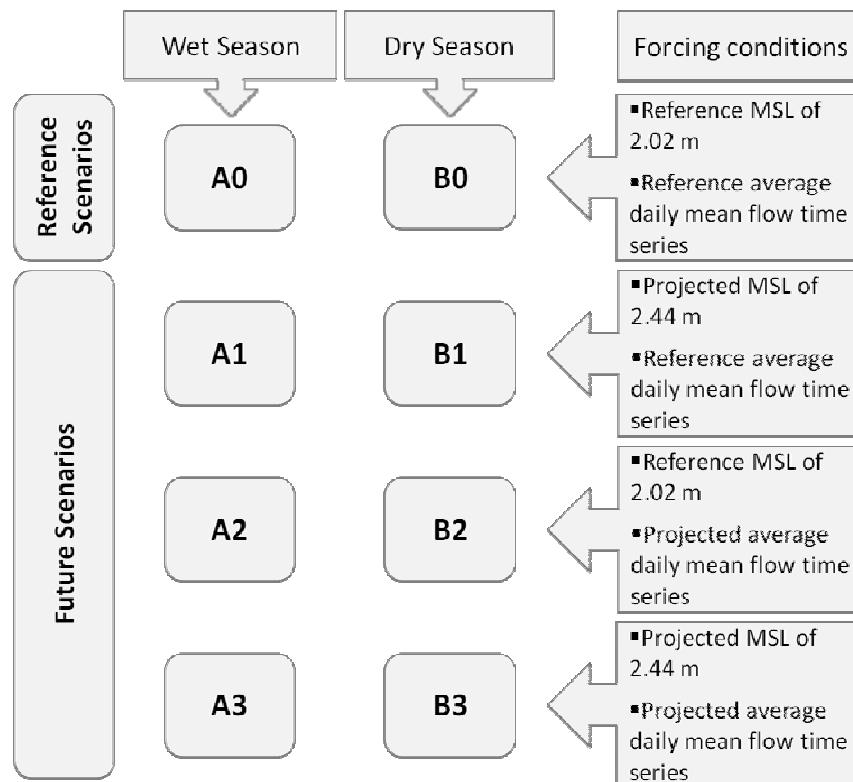
Figure 4.3 Schematic description of the designed scenarios.

Each scenario was simulated for a period of time covering neap tide, spring tide and equinoctial tide. The harmonic constituents imposed at the ocean open boundary were obtained after harmonic analysis (Pawlowicz *et al.*, 2002) of sea surface elevation (SSE) measurements of Barra gauge. Dry and wet seasons are simulated in order to include the spring, neap and equinoctial tide previously referred. The simulation intervals are presented in Table 4.1 and also marked in Figure 4.4. Moreover, to obtain mean salinity maps, helpful in the lagoon physical zonation based in Venice System, a period of mean amplitude tide is also considered (see Table 4.1). These tides were previously identified through the analysis of tidal predictions at Ria de Aveiro mouth for the year 2010.

Table 4.1 Periods and tides amplitude for each tide considered.

Tide	Simulation period	Tidal amplitude (m)
Dry Season		
Equinoctial	9/9 – 10/9	3.55
Spring	24/9 – 25/9	2.55
Neap	16/9 – 17/9	1.35
Mean amplitude	20/9 – 21/9	1.98
Wet Season		
Equinoctial	28/2 – 1/3	3.60
Spring	16/3 – 17/3	2.63
Neap	8/3 – 10/3	1.12
Mean amplitude	12/3 – 13/3	2.08

All scenario simulations were carried out using the same settings considered for the calibration of the hydrodynamic and salt transport models (Sections 5.2 and 5.3), with the exception of the atmospheric forcing. Projected changes in saline patterns and physic zonations according to Venice System are evaluated in Chapter 0.

4.2.1 Local mean sea level

Based in the Cascais tide gauge records, Antunes and Taborda (2009) recently estimated a MSL rise rate of 2.1 +/- 0.1 mm/year for the period 1977-2000 and identified an increase rate from 1.9 mm/year to 2.9 mm/year between 1977 and 2008 for this region. Araújo (2005), analyzing Aveiro tide gauge records, found a relative MSL rise at a rate of 1.2 +/- 0.7 mm/year for the period 1976-2003, the only estimative for this region.

Recent studies point different global MSL rise projections for the end of 21st century. Meehl *et al.* (2007) indicate rises between 0.18 and 0.59 m while Vermeer and Rahmstorf (2009) defends worsening projections between 0.6 and 1.8 m.

The MSL rise value used in this study was estimated by Lopes *et al.* (2011) from GISS-ER model outputs (Russel *et al.*, 1995, 2000). This model is the one of the seventeen Atmosphere Ocean General Circulation Models (AOGCMs) used by IPCC that takes into account more processes responsible for MSL rise, namely: thermal expansion, dynamic change and mass exchange at every grid point (Katsman *et al.*, 2007). To consider the uncertainty associated to projections at small spatial scales Lopes *et al.* (2011) analyzed the behavior of sea level change at eight points in front of the Portuguese coast, concluding that the spatial variability is weak. Given

_____

that the GISS-ER model does not consider the effect of land subsidence, its relative importance to local sea level change was evaluated (Lopes e*t al.*, 2011). Peltier (2004) estimated a rate of -0.07 mm/year due to Glacial Isostatic Adjustment (GIA) for the Portuguese coast, representing 5% of the total change, reason why its contribution was neglected. Hence, a local MSL rise of 0.42 m obtained by Lopes *et al.* (2011) corresponds to the mean value of sea level change for these eight points estimated with model GISS-ER for A2 SRES scenario.

Projections based on the extrapolation of observed local data corroborate the value obtained by Lopes *et al.* (2011). A relative MSL rise between 0.14 and 0.57 m by the year 2100 was predicted by Dias and Taborda (1988). More recently, Antunes and Taborda (2009) projected a rise of 0.47 m with a 95% confidence interval between 0.19 and 0.75 m in the year 2100 relative to 1990 for Cascais.

4.2.2   River flow regime

In order to characterize reference and projected river flow regime of the lagoon main tributaries, and to determine average daily mean flow time series to be used as forcing in the MOHID simulations of the scenarios under study, the daily mean flow time series obtained with the SWAT were used. For the reference conditions, the daily mean flow series obtained from the SWAT model simulations for the period from 1st January 1971 until 31st December 2000 took in account the precipitation series of the IPCC scenario for climate of the 20th century (20C3M scenario) at the nearest point of the study area. For future conditions were considered the daily mean flow series between 1st January 2071 and 31st December 2100, obtained from SWAT model simulations taking into account series of the atmospheric general circulation model ECHAM5 (Roeckner *et al.*, 2003) at A2 SRES scenario.

The annual and seasonal average freshwater inflow into Ria the Aveiro lagoon, for each main tributary at an average year, were calculated in this study based on the results obtained with SWAT model.

The total annual average freshwater inflow into Ria the Aveiro is estimated at about 62 m^3/s. The Vouga river has the largest freshwater contribution, about 77% of the total, followed by the Mira ditches with a contribution of about 13%, and the Antuã river representing about 4% (Table 4.2). The Boco, Caster and Gonde rivers give a smaller contribution. In wet conditions, the total average flow more than doubles the total annual mean flow (about 143 m^3/s), with the various tributaries giving about the same freshwater relative contribution. At dry conditions, the total average flow is negligible if compared with the average annual mean flow (about 1.53 m^3/s).

For the future conditions, is projected a reduction in the annual average freshwater inflow to the lagoon (43 m^3/s), the same occurring for wet and dry seasons (Table 4.3). However this reduction is more significant in the dry season. Indeed, while in the wet season is projected a mean flow decrease of about 32% relatively to reference conditions, in the dry season the seasonal average flow of 0.2 m^3/s reflects a reduction of about 83%. The relative contribution of each tributary remains about the same in annual, wet season and dry season periods.

Table 4.2 Estimative of reference average annual and seasonal mean flow, and each tributary relative contribution.

Tributary	Average annual mean flow (m³/s)	Annual relative contribution (%)	Average wet season mean flow (m³/s)	Wet season relative contribution (%)	Average dry season mean flow (m³/s)	Dry season relative contribution (%)
Caster + Gonde	2.54	4.0	3.04	2.1	0.02	1.3
Antuã	2.72	4.3	6.41	4.5	0.04	2.6
Vouga	47.98	75.8	111.35	77.8	1.01	66.4
Boco	1.99	3.2	4.38	3.1	0.09	5.8
Mira ditches	8.03	12.7	17.88	12.5	0.36	23.9
Total	63.26		143.05		1.53	

Table 4.3 Estimative of future average annual and seasonal mean flow, and each tributary relative contribution.

Tributary	Average annual mean flow (m³/s)	Annual relative contribution (%)	Average wet season mean flow (m³/s)	Wet season relative contribution (%)	Average dry season mean flow (m³/s)	Dry season relative contribution (%)
Caster + Gonde	1.72	4.0	2.33	2.1	0.00	0.4
Antuã	1.86	4.3	4.98	4.5	0.00	0.9
Vouga	32.67	76.2	86.90	77.8	0.11	54.0
Boco	1.32	3.08	3.46	3.1	0.02	9.0
Mira ditches	5.32	12.4	13.97	12.5	0.07	35.7
Total	42.88		111.64		0.20	

Figure 4.4 presents estimated average daily mean flow time series at wet and dry seasons, being marked the equinoctial, neap, mean amplitude and spring tidal periods under study. As can be observed, and in agreement with Tables 4.2 and 4.3, in general an average daily mean flow decreases is projected for the future scenarios.

These estimates were calculated in the scope of this study in order to obtain river flow daily series for each season, representative of a reference and future average year, to be used as forcing in the MOHID water landward boundaries for each scenario simulation. The average daily mean flow corresponds to the average of the thirty daily mean flows for each day of the time series being considered. If, by one hand, the determination of daily series allows to obtain more realistic simulation results along each season, the comparison of results between tidal periods at each scenario is not so well succeeded, due to the flow variability along the time series. Alternately it could have been considered a constant mean flow value as forcing for the season.

When comparing reference and future daily mean flow series (Figure 4.4) a river flow decrease in the region is projected for both wet and dry seasons.
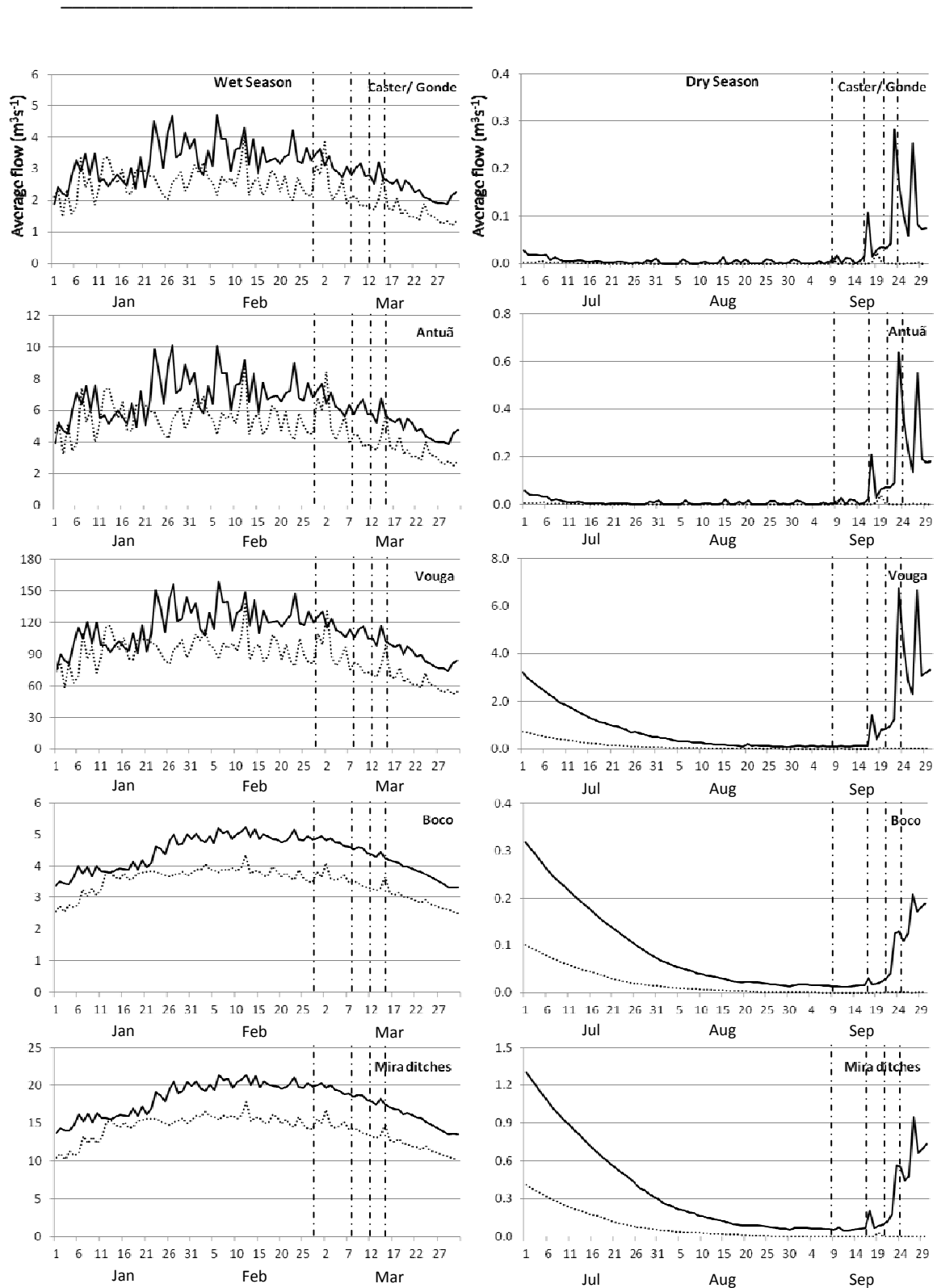
Figure 4.4 Estimated average daily mean flow for wet and dry seasons at the main Ria de Aveiro tributaries (solid line: flow in reference conditions; dotted line: flow in projected conditions; 1st dashed-dotted line: equinoctial tide; 2nd dashed-dotted line: neap tide; 3rd dashed-dotted line: mean amplitude tide; 4th dashed-dotted line: spring tide).

_____

# 5 Model design and calibration

5.1 Numerical grid improvement

In shallow water systems like Ria de Aveiro, apart from boundary conditions, bathymetry is probably the determinant factor affecting its hydrodynamic. The bathymetry influences the spatial variability of the current magnitude and direction, constituting a factor which ensures the realism of the numerical model (Cheng *et al.*, 1991; Dias and Lopes, 2006).

Mendes *et al.* (2011) carried out a hydrodynamic modeling study to compare the performance of the MOHID hydrodynamic model when including the low lying lands surrounding the Aveiro lagoon, taking into account that these areas will probably be frequently flooded in the near future (Nicholls *et al.*, 2007). For this objective accomplishment, two different numerical bathymetries were considered: one comprising data until 4 m and other until 9 m above the chart datum. Negligible differences were identified in the numerical results for the general circulation. Though, low lying areas should be included in order to evaluate MSL rise or flooding effects.

Vaz *et al.* (2007a) begun to develop the numerical bathymetry taken as a starting point for this study. These authors considered for this propose a general survey, carried out in 1987/88 by the Hydrographic Institute of Portuguese Navy (IH), and included field data updates from several surveys performed by the Aveiro Harbor Administration (APA) at the inlet channel and close to the lagoon's mouth, from the 1998 and 2002 dredging operations. The numerical grid developed by Vaz *et al.* (2007a) has 567 by 438 cells in the *y* and *x* directions, respectively, with a spatial resolution of 40×40 m in the central area of the lagoon and of 40x100 m in the north and south areas of the lagoon. The lagoon's complex geometry, especially the lagoon central zone where the channels are very narrow, and the consequent decrease in computational effort, justifies the variable spatial step considered (Vaz *et al.*, 2007a).

A recent version of this initial numerical bathymetry was then obtained including topographic data provided by Intermunicipality Community of Ria de Aveiro (CIRA) relative to the year 2006, in order to take into account low lying adjacent lands. This numerical bathymetry was also updated with data from: surveys conducted by APA at the inlet in 2003; topo-hydrographic surveys conducted by ARH Centro in 2010; Polis Litoral Ria de Aveiro for 2011, covering channel's banks, and Ílhavo and Mira channels; and APA surveys performed until 2010.

The numerical bathymetry described above was updated (Figure 5.1 A)) in the scope of this study with recent surveys from Aveiro Harbor Administration (APA), dating from February 2012, and comprising the area under APA jurisdiction. This recent data was firstly interpolated with an algorithm whose principle consists in ensuring water volume conservation in each cell of the future numerical bathymetry - the Monte Carlo cubature method (Dias, 2001). A second interpolation was performed, using the Kriging method from the Surfer® software, to fill the cells without values. Finally it was only necessary to replace the updates in the numerical bathymetry taken as work base. Grid cells above 10 meters relative to the chart datum were removed.
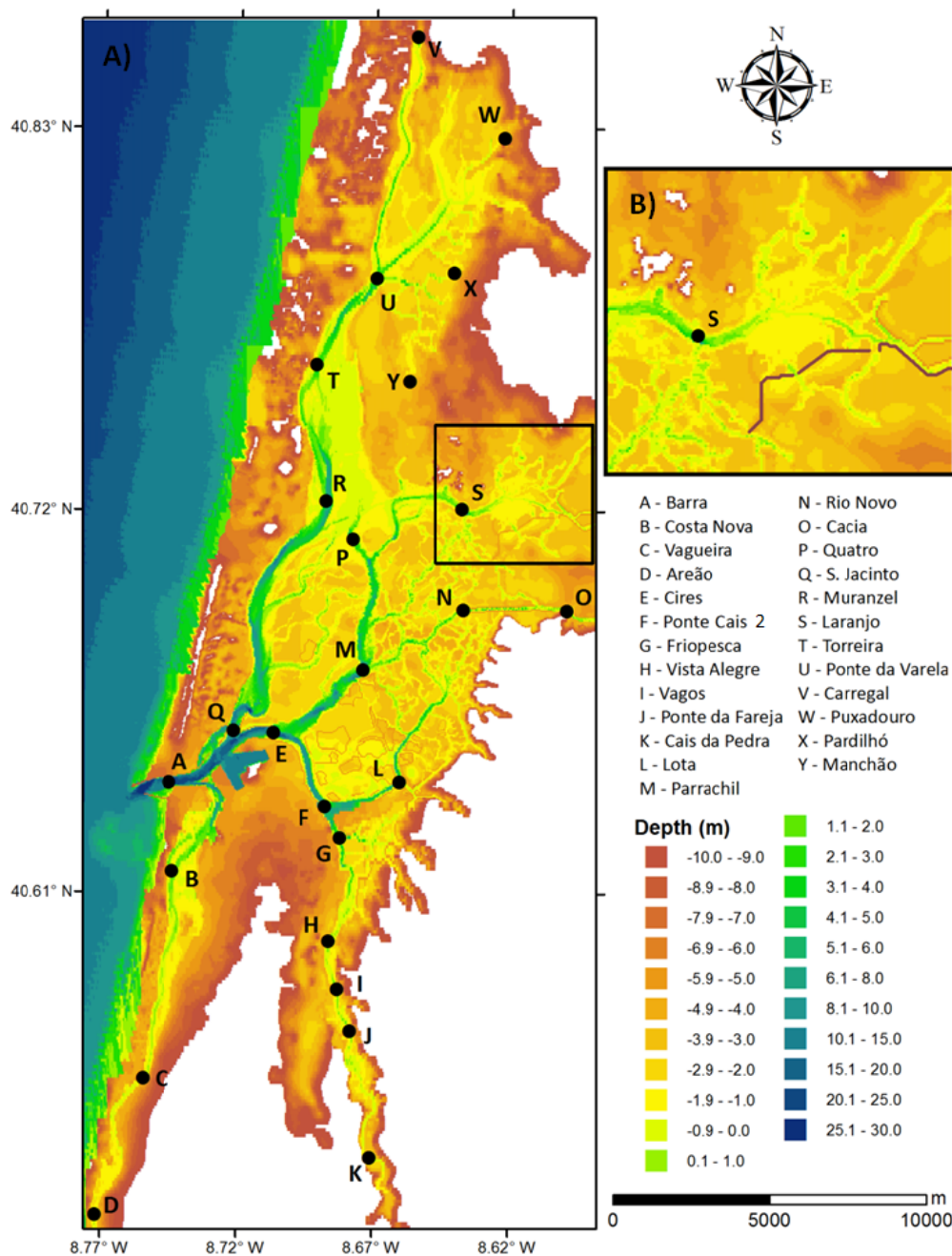
Figure 5.1 A) Numerical grid of the Ria de Aveiro lagoon with locations of the stations where field data is available; B) Detail of the Baixo Vouga dike.

The updated bathymetry was improved reintroducing missing structures, absent due to the mesh resolution, and elevating other ones, whose height was attenuated as a consequence of the interpolation procedure. Comparing the numerical bathymetry with actual orthophotos in ArcGIS environment, walls of active salt pans, dikes (Figure 5.1 B)) and roads bordering the lagoon next to main settlements (Aveiro Harbor, Gafanha da Nazaré, Aveiro, Ílhavo, Torreira, S. Jacinto and Vagueira) where identified, redesigned and given more realistic levels. This procedure intended to confine the lagoon water expansion (resulting from projected sea level rise, storm surges and river floods) to the effectively potential flooding areas. Assuming that salt pans will remain in

operation and the protective function of dikes and roads/walls will be preserved till the end of the XXI century, levels of 5 m above the chart datum were attributed to the salt pans walls, to the bordering roads, and to the Baixo Vouga dike.

5.2 Hydrodynamic model calibration and validation

Estuarine numerical models are tools for reconstructing real phenomena occurring in these systems. Before using them in a practical application their calibration and validation with independent data is required. The model calibration is based on the adjustment of parameters to which the model is most sensitive. It is frequently made by comparing short time series of predicted and measured data for the same location and period of time (Cheng *et al.*, 1993). Smith (1977) suggests another method, specific for hydrodynamic model calibration, consisting in the comparison of harmonic constituents generated from predicted and observed data. The model validation is a procedure to test the model predictions accuracy when compared with measurements independent from the data set used in calibration (Dias *et al.*, 2009).

5.2.1   Calibration

According to Dias and Fernandes (2006), the magnitude of the bottom friction coefficient determines changes in the tidal wave propagation within Ria de Aveiro lagoon, resulting in a tidal energy damping as it propagates from the mouth of the lagoon towards the end of the channels. Therefore, the model parameter tuned, in order to perform the hydrodynamic model calibration, was the Manning coefficient (n) (Equation 4.8). In this study, a Manning coefficient grid developed by Vaz *et al.* (2007a), previously locally fine-tuned based on the Hsu *et al.* (1999) procedure was used.

Model calibration was carried out by comparing predicted and observed time series of sea surface elevation (SSE), and by comparing the amplitude and phase of the harmonic tidal constituents. For this effect sea surface elevation data from the most recent tide survey conducted in Ria the Aveiro (carried out between 2002 and 2003) were used. These data were surveyed by Araújo (2005) in the scope of a PhD Thesis. The measurements were performed every six minutes, except in station T (see Figure 5.1) where measurements were performed every half hour.

At the open ocean boundaries, 36 tidal harmonic constituents obtained from harmonic analysis (Pawlowicz *et al.*, 2002) of SSE time series measured during 2002 at Barra tide gauge (station A) were imposed. A correction factor was applied to phase and amplitude of the major harmonic constants imposed in the ocean open boundary so the model results reproduce the free surface elevation at the tidal gauge. As hydrodynamic model was only forced by tides, in order to compare model results with measurements the low frequency signal was removed from the data considering a cut-off frequency of 0.0000093 Hz (30 h).

Values of 7.5 s for time step were adopted and 5 m^3s^{-1} for horizontal eddy viscosity. Null free surface elevation and null velocity were used as initial conditions for the hydrodynamic model in all grid points. The model was spun up from rest over 3 days in order to guarantee the stability of the results and their independence from the initial conditions.

The model performance is evaluated following the methodology proposed by Dias and Lopes (2006), consisting in determine Root Mean Square (RMS) (Equation 5.1) and Skill parameter (Equation 5.2):

$$RMS = \left\{ \frac{1}{N} \sum_{i=1}^{N} [\zeta_0(t_i) - \zeta_m(t_i)]^2 \right\}^{1/2} \tag{5.1}$$

$$Skill = 1 - \frac{\sum |\zeta_m - \zeta_0|^2}{\sum [|\zeta_m - \overline{\zeta_0}| - |\zeta_0 - \overline{\zeta_0}|]^2} \tag{5.2}$$

where $\zeta_0(t_i)$ and $\zeta_m(t_i)$ are the observed and modeled SSE, respectively, and N is the number of measurements in the time series.

According to Dias *et al.* (2009) the RMS values should be compared with the local tidal amplitude. If RMS is lower than 5% of the local amplitude, the agreement between model results and measurements should be considered excellent. If it ranges between 5% and 10% the agreement is then considered very good.

The model predictive Skill quantitatively evaluates the agreement between model results and observations, and was developed by Wilmott (1981) and recently used by Warner *et al.* (2005), Li *et al.* (2005) and Vaz *et al.* (2009). Perfect agreement between model results and observations yields a Skill of one, and complete disagreement yields a Skill of zero. Skill values higher than 0.95 should be considered representative of an excellent agreement between model results and observations (Dias *et al.*, 2009).

Predicted and observed SSE time series is shown Figure 5.2 for the 18 stations considered for the calibration procedure.

The RMS, compared with mean local tidal amplitude, and Skill were determined for each station and are presented in Table 5.1. The results reveal an accurate reproduction of SSE in the central area of the Ria de Aveiro lagoon, along the Espinheiro channel and in the Laranjo basin. The RMS values range from 2.5% to 10% of the mean tidal amplitude at stations A, B, E, F, H, L, Q and T, closest to the lagoon mouth, and in station O, at the Espinheiro channel's head (Figure 5.2 presents predicted and observed SSE series for stations A, H, O, Q and T). Stations A (Barra), B (Costa Nova) and Q (S. Jacinto) present an excellent agreement between predictions and observations, while the others six show a very good agreement.

At station A the agreement between model results and data should be perfect. However this is not the case. A RMS error of about 6 cm was found at the mouth of the lagoon, representing less than 3% of the mean tidal range. This difference may be justified by an inaccurate phase and amplitude correction factor for the major tidal constituents imposed at the open ocean boundary. This small error may partially explain the errors found in the other stations.

In general, disagreement between model results and data increases with the distance from the lagoon's mouth. This disagreement is higher for station K located near the Ílhavo channel's head, with a RMS representing about 24% of the mean tidal range, and for station V close to S. Jacinto channel's head, where RMS corresponds to about 26% of the mean tidal range.

Other important error source is the inaccurate definitions of the numerical grid. For example, at the end of Ílhavo channel there is a very narrow section with a width of about 10 m which is very difficult to represent in the numerical grid, even with cells of 40 m wide. This may explain the disagreement found at station K.
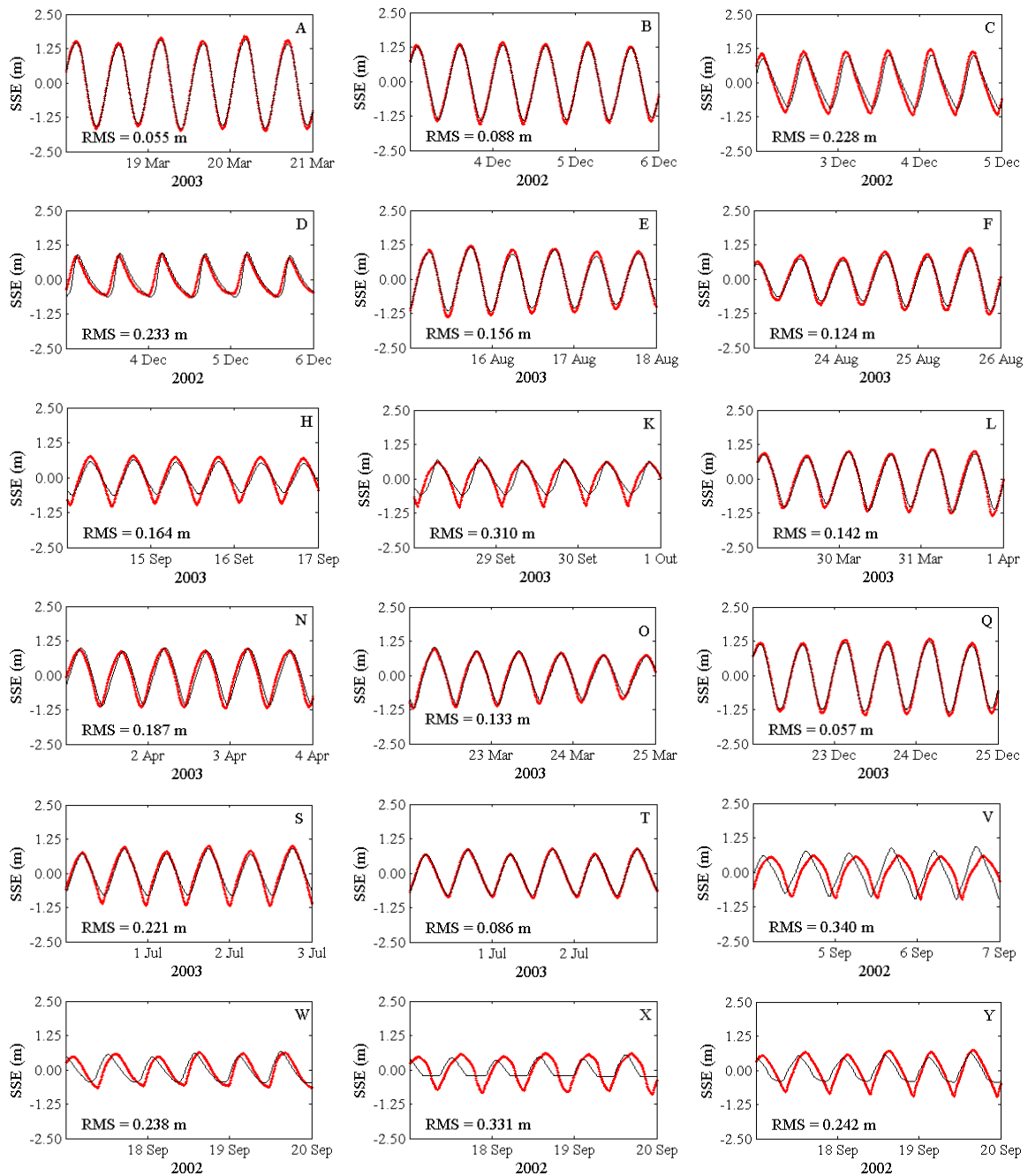
Figure 5.2 Comparison between predicted and observed SSE series for the stations used in the hydrodynamic calibration procedure (black line: measurements; red line: model results).

In general, Skill values are higher than 0.95, except in stations farther from the inlet (D, K, V, W, X and Y).Therefore, an excellent agreement between model results and observations is achieved in the lagoon's central area till the main channels middle sections.

Table 5.1 RMS, RMS relative to mean local tidal amplitude and Skill for all the stations used in hydrodynamic calibration procedure.

Designation	Station	RMS (m)	RMS relative to mean local tidal amplitude (%)	Skill
Barra	A	0.055	2.47	0.999
Costa Nova	B	0.088	4.63	0.996
Vagueira	C	0.228	12.68	0.957
Areão	D	0.233	21.16	0.908
Cires	E	0.156	9.15	0.989
Ponte do Cais	F	0.124	6.55	0.992
Vista Alegre	H	0.164	8.63	0.966
Cais da Pedra	K	0.310	23.82	0.846
Lota	L	0.142	7.27	0.989
Rio Novo	N	0.187	11.02	0.975
Cacia	O	0.133	8.89	0.985
S. Jacinto	Q	0.057	2.87	0.998
Laranjo	S	0.221	12.26	0.962
Torreira	T	0.086	5.7	0.993
Carregal	V	0.340	26.17	0.851
Puxadouro	W	0.238	21.63	0.915
Pardilhó	X	0.331	20.68	0.809
Manchão	Y	0.242	16.71	0.921

The direct comparison of RMS errors and Skill parameter has the disadvantage of quantifying together phase and amplitude errors. Thus, harmonic analysis (Pawlowicz *et al.*, 2002) was performed for both predicted and observed SSE in order to quantify separately the amplitude and phase lags for all stations.

Results for the major semi-diurnal and diurnal constituents (M_2 – 12.42 h; S_2 – 12 h; N_2 – 12.9 h; K_1 – 23.93 h; O_1 – 25.82 h), and for the shallow water constituent (M_4 - 6.21 h) are presented in Figure 5.3.

The agreement between predicted and observed values for the two major semi-diurnal tidal constituents in Ria de Aveiro (M_2 and S_2) is rather good, for both amplitude and phase. Stations D, S, V and W reveal the higher discrepancies in the M_2 amplitude, while the higher discrepancies in the M_2 phase are identified for stations C, D, K and N, when compared with other stations.

For the M_2 constituent, the mean difference between predicted and observed amplitudes is about 9 cm and the mean phase difference is about 12°, which means that the average delay between the predicted and observed tide is about 25 minutes. For the S_2 constituent, the mean amplitude deviation is about 3 cm and the phase difference of about 23° (corresponding to an average delay of 45 minutes). For the diurnal constituents K_1 and O_1 the mean amplitude difference, compared with the mean constituent amplitude is of about 21% and 10%, respectively. Regarding the phase of these constituents, the mean difference is about 41° (85 minutes) and 72° (150 minutes), respectively. The model forecasts show that the M_4 harmonic constituent reproduction is not as accurate as for the other constituents. This can be explained by the lower quality of the topographic data. The M_4 mean amplitude difference for all stations is about 3.4 cm

(50% of the mean amplitude) and the phase delay is about 60°, which represents 61 minutes. Nevertheless, the results for the M_4 constituent are considered accurate to perform this work.
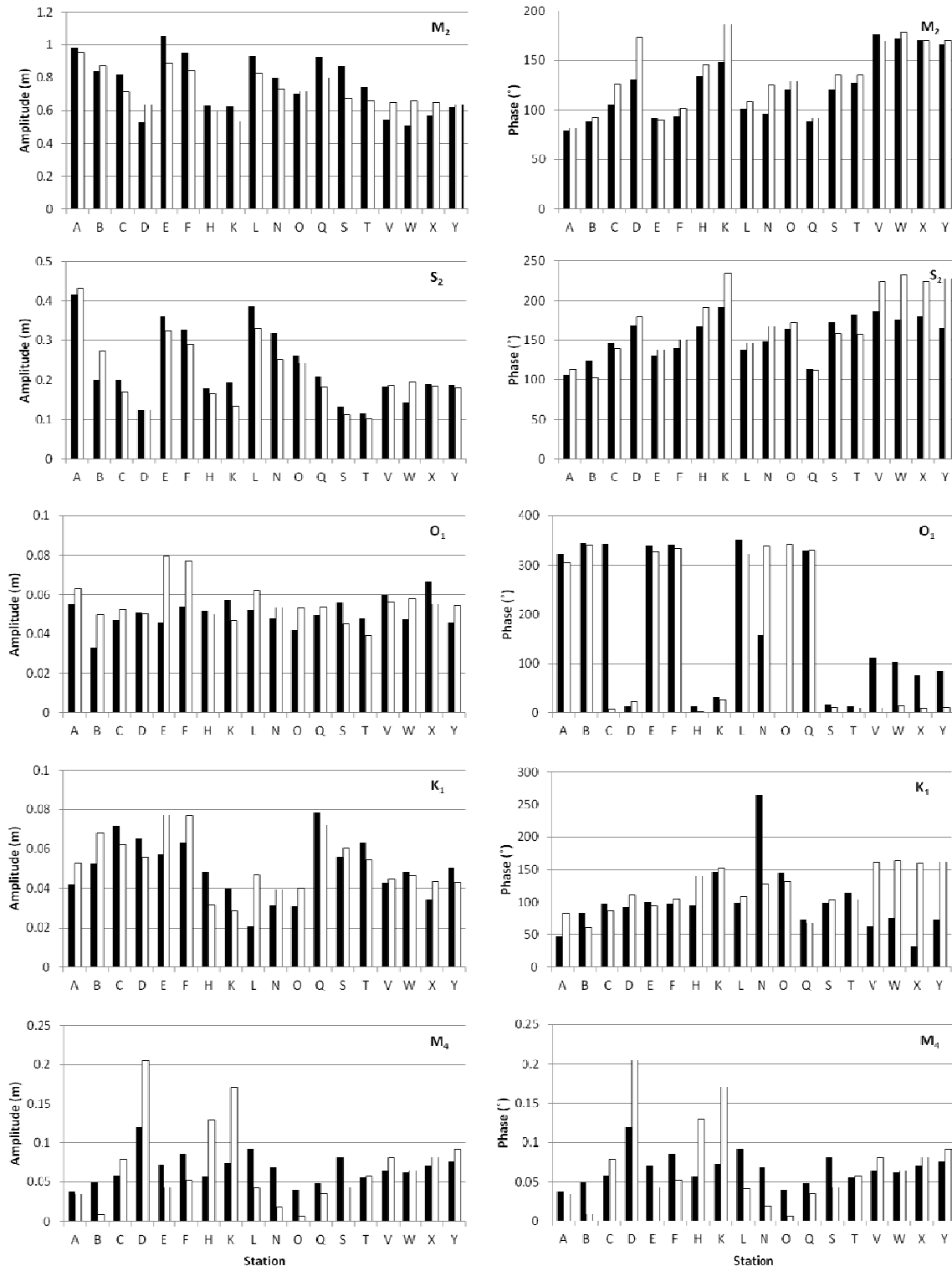

Figure 5.3 Comparison between predicted and observed amplitude and phase for M_2, S_2, K_1, O_1 and M_4 harmonic constituents (black bars: measurements, white bars: model results).

According to these results, and in spite of the differences between model predictions and field data, the model can be considered successfully calibrated.

5.2.2 Validation

The model performance was evaluated for a period during June 1997, taking into account the availability of field data, by comparing modeled and observed data of SSE and current velocity at ten stations distributed along the main channels of the lagoon (their location is shown in Figure 5.1).

The validation procedure was carried out without changing the Manning coefficient grid used during the calibration and with the same tidal forcing in the ocean open boundary. Figures 5.4 and 5.5 show modeled and measured along-channel SSE and velocities time series, respectively.

SSE predicted and observed time series show a pattern similar to the obtained for the calibration procedure (Figure 5.4).

Figure 5.4 SSE time series for stations Q, B, C, U, R, P, G, I and J, respectively from left to right and top to bottom (solid line: model results; points: measurements).

The RMS errors for SSE range from 3 to 8% at seven stations (B, G, H, I, P, Q and R) and around 11% in Vagueira and Ponte da Fareja stations. The error is relatively higher in Ponte da Varela, of 27%. The larger discrepancies occur upstream Mira, São Jacinto and Ílhavo channels (Table 5.2), which can be due to the greater distance from the mouth that induces a phase lag increase and, in the case of Ponte da Fareja station also due to the very narrow stretch at the end of Ílhavo channel, which is not well resolved by a model using grid cells 40 meters wide. Except for the last three stations, the agreement between values is rather good, revealing that a general agreement was achieved between computed and measured SSE.

Table 5.2 RMS, RMS relative to mean local tidal amplitude and Skill of SSE for all the stations used in hydrodynamic validation procedure.

Designation	Station	RMS (m)	RMS relative to mean local tidal amplitude (%)	Skill
Costa Nova	B	0.111	4.45	0.995
Vagueira	C	0.175	10.56	0.980
Friopesca	G	0.139	5.56	0.992
Vista Alegre	H	0.122	6.24	0.991
Vagos	I	0.055	4.81	0.995
Ponte da Fareja	J	0.117	10.81	0.967
Quatro	P	0.127	7.94	0.986
S. Jacinto	Q	0.067	3.26	0.998
Muranzel	R	0.140	6.82	0.986
Ponte da Varela	U	0.303	27.02	0.893

Considering that most of the lagoon's channels are aligned along a main direction, in order to compare the velocities, the main flow direction for measurements and predictions was determine at each station. These directions were almost coincident and the modeled and measured current velocities were projected along them. The across-channel flow velocities were not analised, because they were considered negligible.

Discrepancies between the model results and the field data are well observed when assessing velocities point by point (Figure 5.5).

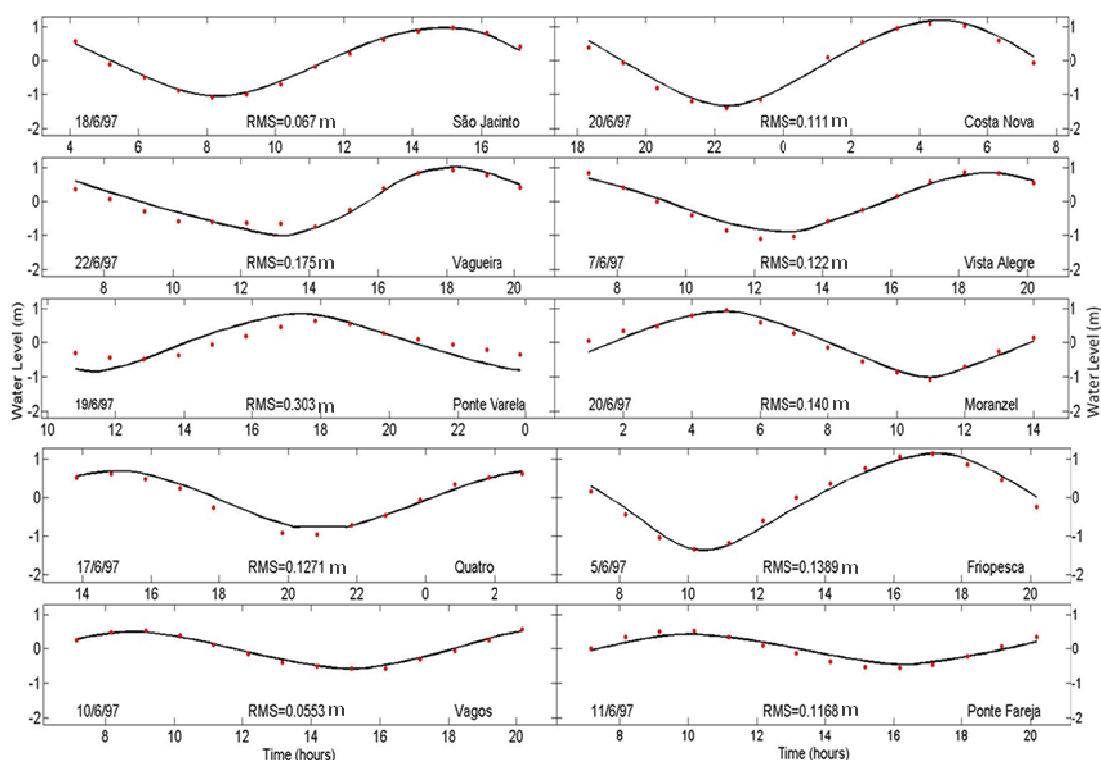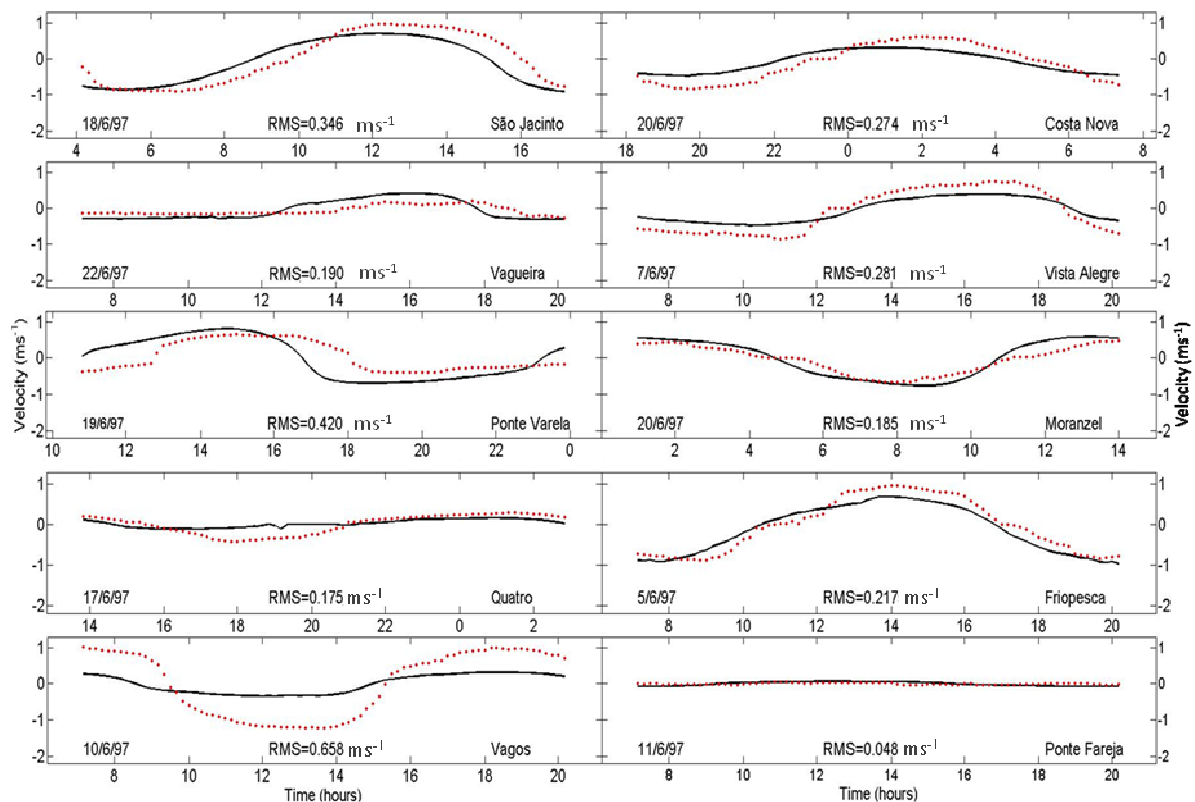**Figure 5.5 Time series of current velocity for stations Q, B, C, H, U, R, P, G, I and J, respectively from left to right and top to bottom (solid line: model results; points: measurements).**

Larger differences then those obtained for SSE are found for current velocity. The RMS errors reach values as high as 0.7 m/s in station I. Indeed, RMS errors relative to current velocity local range are very high, varying from about 12% in station G and 44% in station J (Ponte da Fareja). The larger value in station J may be related with the lower magnitude of the current velocity in this station and also doe to the very narrow stretch at the end of Ílhavo channel, as referred above. The errors of 41% in Vagueira station, 30% in Vagos station and 40% in Ponte da Varela station can be due to the greater distance from the mouth, inducing a phase lag increase. Stations located near the lagoon mouth, in the lagoon central zone, show RMS relative errors not larger than 20%, presenting a relatively good reproduction of current velocity field measurements.

Table 5.3 RMS, RMS relative to current velocity local range and Skill of current velocity for all the stations used in hydrodynamic validation procedure.

Designation	Station	RMS (m/s)	RMS relative to current velocity local range (%)	Skill
Costa Nova	B	0.274	19.01	0.877
Vagueira	C	0.190	41.33	0.767
Friopesca	G	0.217	11.76	0.969
Vista Alegre	H	0.281	17.30	0.905
Vagos	I	0.658	29.51	0.668
Ponte da Fareja	J	0.048	44.47	0.611
Quatro	P	0.175	24.39	0.705
S. Jacinto	Q	0.346	18.34	0.927
Muranzel	R	0.185	16.24	0.955
Ponte da Varela	U	0.420	39.96	0.800

SSE model results reveal a good reproduction of the observed data set for the generality of the lagoon's stations, despite a not so good reproduction of current velocity. Therefore, it may be considered that the model reproduces with good accuracy the SSE data for these stations, concluding that the hydrodynamic model is validated.

5.3 Salt and heat transport model calibration

The salt transport model is coupled with the hydrodynamic model already calibrated and validated for the Ria de Aveiro. Salt and heat transport model is calibrated by comparing measured and predicted salinity and water temperature time series for seven stations distributed along the main lagoon channels (station locations in Figure 5.1). Although the main objective of this thesis dispense the heat transport model application, its calibration is carried out taking into account that this model is intended to be used in the scope of future work.

With this purpose, a data set of salinity and water temperature measurements was considered. These measurements were performed every hour during a period of 25 hours in July 1996 (from 09/07/1996 to 28/07/1996). These observations were carried out after a long dry period, with a lower river flow contribution. As meteorological input, data concurrent with the simulation period was considered from the NCEP data base (nearest grid point: 40.953°N, -9.375°W). On the ocean open boundary were imposed constant values of salinity (36.5 - the same

_____

adopted by Vaz *et al.* (2009), and by Mendes (2010)) and a water temperature value of 15.2 °C. This temperature value corresponds to the temperature average considering the superficial one hundred meters of the oceanic water column in the lagoon's nearest point (40.5°N e 9.5°W) of the Levitus climatological data base (Boyer *et al.*, 2009). Landward boundaries were forced with SWAT model results for river flow and water temperature (daily time series) coincident with the period of interest. It is noted that in previous studies the river flow was imposed constant for the main tributaries (Vaz *et al.*, 2005; Mendes, 2010). Salinity values were specified as 0. A value of 5 m^2s^{-1} was adopted for both salt and heat diffusion coefficients.

The model was spun-up for a time period of about two times the maximum residence time found by Dias (2001) for the upstream regions of the Ria de Aveiro lagoon. The spin-up time was about 40 days. This time period was considered adequate to reach a thermohaline equilibrium within the Ria de Aveiro lagoon. The calibration period was simulated *in continuum* once finished the spin-up period.

Figures 5.6 and 5.7 compare modeled and measured salinity and water temperature time series at each station considered for calibration period. The adjustment was quantitatively assessed by determining RMS (Equation 5.1) and Skill (Equation 5.2) for all the stations.

The agreement between predicted and measured salt concentration time series is very good. The salinity data is well reproduced in almost all stations, with results revealing small differences in phase and amplitude when compared with data, exception made to station U whose results present significant lower amplitude and lag relative to data (Figure 5.6).
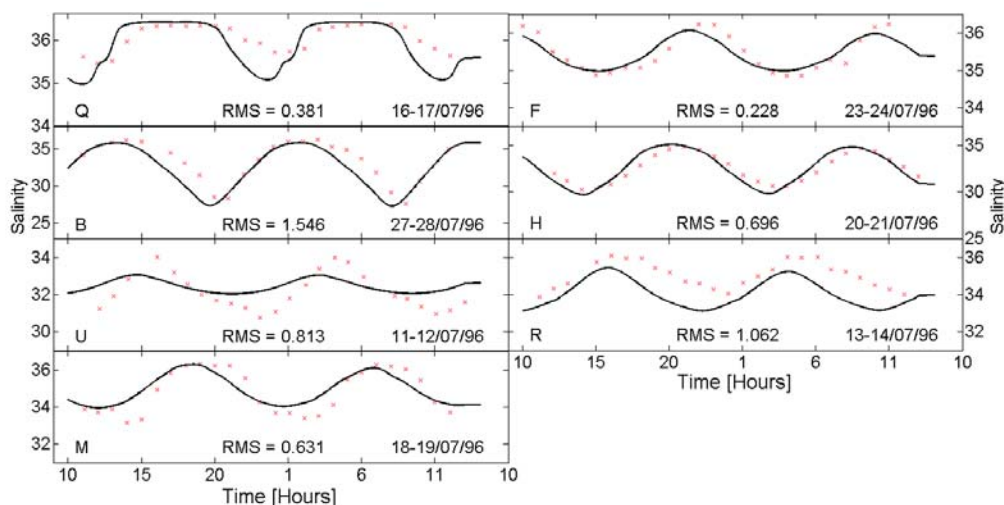
Figure 5.6 Comparison of salinity time series for the stations used during the calibration procedure (solid line: measurements; points: model results).

The RMS values are lower than 5% of the mean local salinity range for all the stations considered (Table 5.4). The stations B and R present the higher RMS values, 1.5 (about 5% of the mean salinity) and 1.1 (about 3% of the mean salinity), respectively. Despite presenting a relative good RMS value, station U shows the larger discrepancy in Skill. Forcing the model with river flow time series, gave the model the ability to reproduce salinity variations more accurately than in

previous studies, where the river flow were imposed constant for the main tributaries (Vaz *et al.*, 2005; Mendes, 2010).

Table 5.4 RMS, RMS relative to mean local salinity range and Skill of salinity for all the stations used in salt transport calibration procedure.

Designation	Station	RMS	RMS relative to mean local salinity range (%)	Skill
Costa Nova	B	1.546	4.63	0.920
Ponte do Cais	F	0.228	0.64	0.928
Vista Alegre	H	0.696	2.14	0.955
Parrachil	M	0.631	1.81	0.886
S. Jacinto	Q	0.381	1.06	0.782
Muranzel	R	1.062	3.03	0.641
Ponte da Varela	U	0.813	2.53	0.605

The comparison between the model results and water temperature data (Figure 5.7) shows a relatively good agreement. Indeed, 50% of the stations present RMS values between 5% and 10% of the mean local temperature range – stations B, F, H and R (Table 5.5). Stations M and Q show higher discrepancies between model results and data, of about 2.3°C and 3.6°C, respectively. Modeling results are overestimated comparatively to data. These discrepancies may be related with river water temperature forcing at the land boundaries. Several other variables can introduce errors, like: the numeric grid resolution and not considering the spatial variations of meteorological data input.

According to these results the model is able to reproduce with good accuracy the salt and heat transport processes in the Ria de Aveiro.
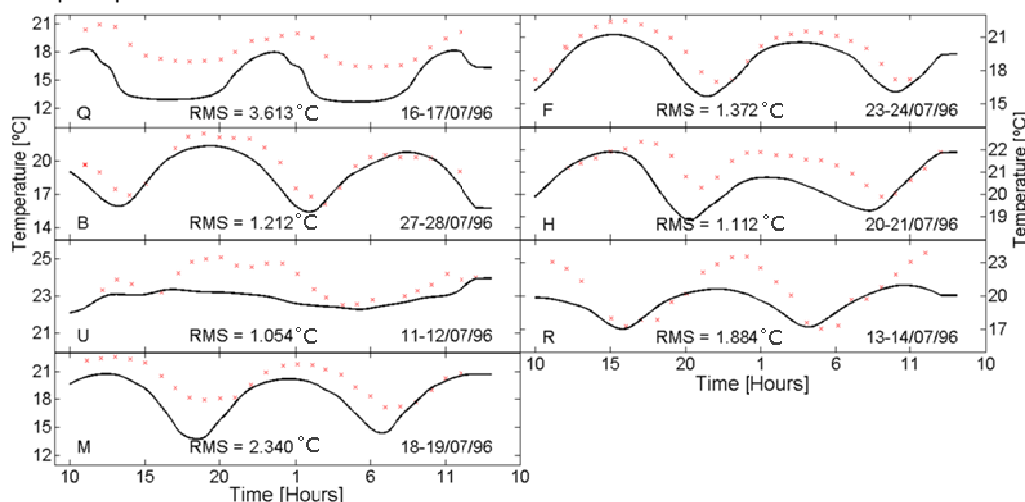
Figure 5.7 - Comparison of water temperature time series for the stations used during the calibration procedure (solid line: measurements; points: model results).

_____

Table 5.5 RMS, RMS relative to mean local temperature range and Skill of water temperature for all the stations used in heat transport calibration procedure.

Designation	Station	RMS (˚C)	RMS relative to mean local temperature range (%)	Skill
Costa Nova	B	1.212	6.16	0.892
Ponte do Cais	F	1.372	6.89	0.869
Vista Alegre	H	1.112	5.22	0.614
Parrachil	M	2.340	11.68	0.715
S. Jacinto	Q	3.613	19.75	0.507
Muranzel	R	1.884	9.15	0.732
Ponte da Varela	U	1.054	4.42	0.583

_____

6 Climate change influence on salt patterns: discussion

In this Chapter the main results obtained are presented and discussed to respond to this thesis objectives. Firstly the maximum salinity changes along the main channels (Section 6.1) are analyzed. Special attention will be paid to possible adaptations in salinity distribution at Espinheiro Channel. In Section 6.2 the adjustments of the salinity fields over the whole lagoon are analyzed, anticipating possible reasons. Finally, modeled reference and projected seasonal zonations (wet and dry seasons) are compared to evaluate the redistribution of the physical zonations. The methodological assumptions presented in Section 4.2 will be taken into account to guarantee a correct interpretation of the analysis developed in the next sections.

6.1 Salinity along channels

The maximum computed salinity from each of the scenarios, being studied in different tidal conditions, was extracted in multiple stations along the lagoon's main channels (Figure 6.1) to allow a quantitative analysis of the projected future seasonal adjustments.
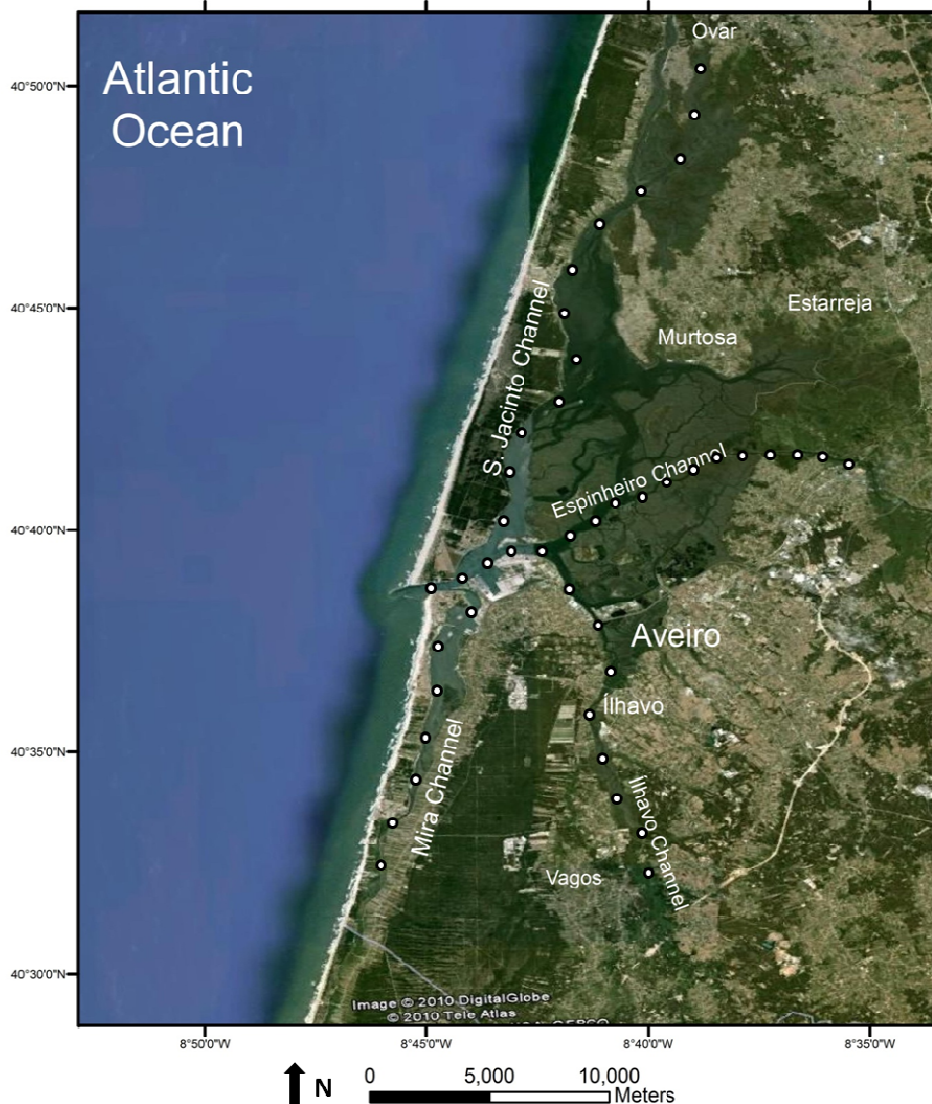
Figure 6.1 Stations location along the main channels.

Figure 6.2 represent the maximum salinity along the main channels obtained in neap and equinoctial tide from reference and projected scenarios (A0, B0, A3 and B3). Just scenarios A3 and B3 are considered in this comparison as they represent the more realistic ones and also able to leverage greater saline intrusion. In wet season is observed, for all the channels, a landward displacement of the saline fronts in A3 scenario, over one to three km depending on the channel and tide.
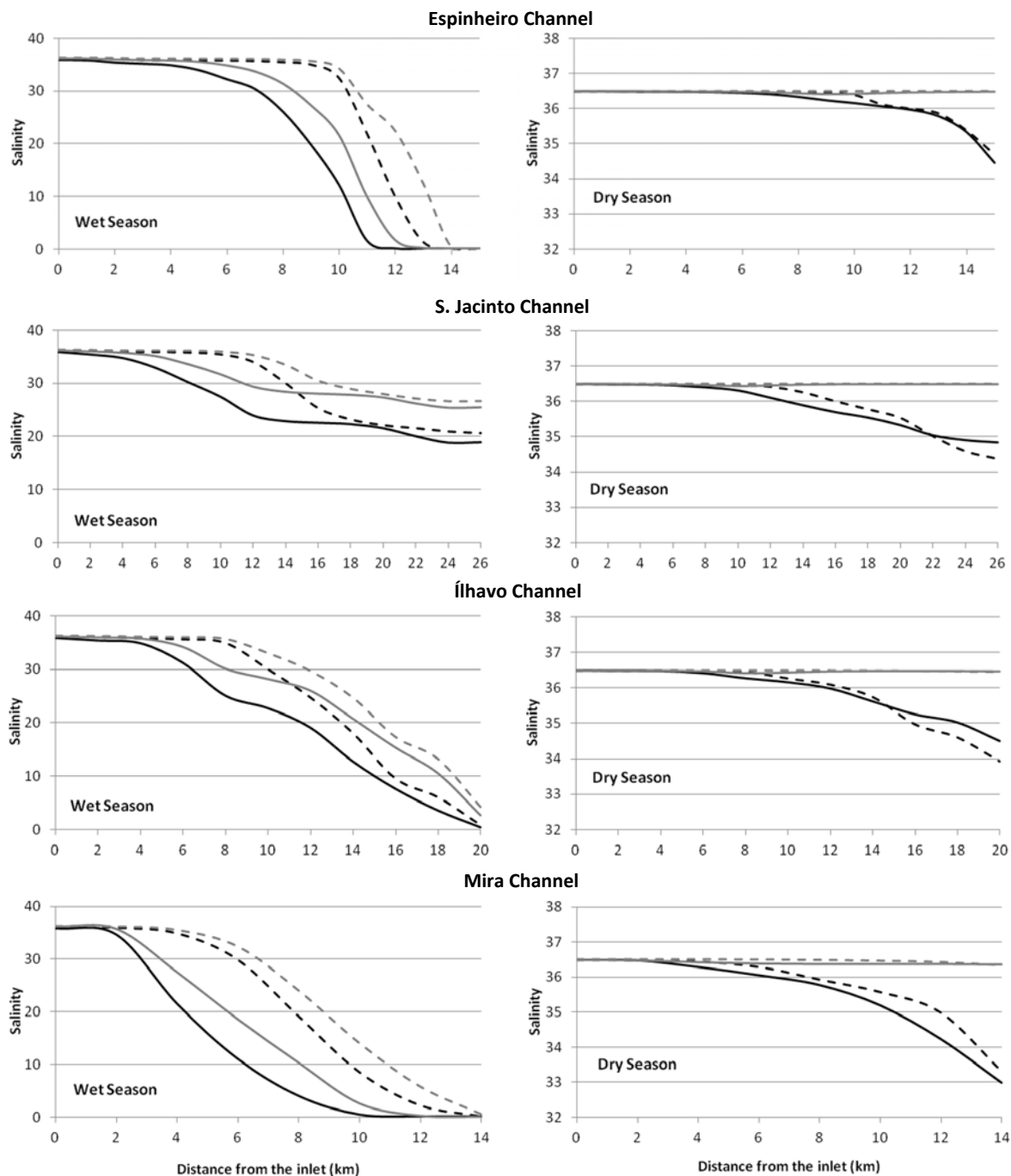
Figure 6.2 Maximum salinity along the main channels for neap and equinoctial tide at A0 and A3 scenarios (wet season), and at B0 and B3 scenarios (dry season) (black solid lines: reference scenarios at neap tide; black dashed lines: reference scenarios at equinoctial tide; grey solid lines: future scenarios at neap tide; grey dashed lines: future scenarios at equinoctial tide).

_____

This landward progression should be due to the combined effect of the MSL rise and river flow reduction as seen in Figure 4.4. It is noteworthy that the variation in the saline fronts position due to the tidal amplitude variability is of greatest importance at any channel under study, comparatively to climate change effects. In fact, from neap to equinoctial higher levels, these fronts vary between two and four km, both for reference and future scenarios.

Analysis of Figure 6.2 for dry season also shows an approximation of the neap tide patterns in the A3 future scenario to the equinoctial tide patterns in the A0 reference scenario. This will lead to, for example, an upstream migration of freshwater intolerant species, the same occurring with salt intolerant species, as a greater lagoon extension will be frequently filled with saltier waters.

In the dry season, with negligible river flow, these fronts are negligible and only denoted in the channel's heads. It is worth noting that in projected conditions the salinity concentrations remain approximately the same from the inlet to the channel's heads (Figure 6.2). In fact, in the equinoctial and neap tidal periods considered the tributaries present a negligible flow for projected scenarios (Figure 4.4).

The Vouga River, with the largest contribution of freshwater inflowing into the Ria de Aveiro during most of an average year, discharges in the Espinheiro channel headwater. According to Table 4.2 the estimated annual mean flow for reference conditions (about 48 m^3/s) represents about 75% of the total mean flow to the lagoon in an average year. For this reason, in this channel are expected the greater longitudinal salinity gradients occurring in the lagoon, justifying largely the Ria de Aveiro classification as a typically estuarine environment.

So, follows an analysis of the saline distribution adjustment along the Espinheiro channel, induced by the scenarios established. The plots of maximum salinity distribution analysis for each scenario at wet season (Figure 6.3) reveal again an upstream advection of the saline front from present to projected conditions. The A3 scenario, combining MSL rise and river flow reduction projections, shows the most significant landward progress of this front (about 1.5 km at equinoctial and spring tide, and 1 km at neap tide), followed by A1 scenario (about 0.75 km in all tidal periods). A reduction is observed on the salinity gradient of the front from the Equinoctial (about 8.0 km^{-1}) to the neap tide (about 4.5 km^{-1}). Figure 6.3 also shows that saline front progresses landward from tides with lower amplitude to tides with higher ones, in accordance with Vaz *et al.* (2005) as referred in section 3.2. For neap tides these fronts are found between 5th and 11th km at reference conditions, and between 5th and 12th km for projected conditions. For equinoctial tides they are found between 10th and 13th km at reference conditions, and between 10th and 14th km for projected conditions. The tidal amplitude, and, in same extent, the combined effect of the river flow variability, determines the position of the saline front and has influence in its salinity gradient.

Analyzing the plots of salinity difference along Espinheiro channel (Figure 6.3), A1 scenario induces a higher salinity increase than A2 scenario, being identified a maximum difference of 8 and 6 at spring tide, respectively.
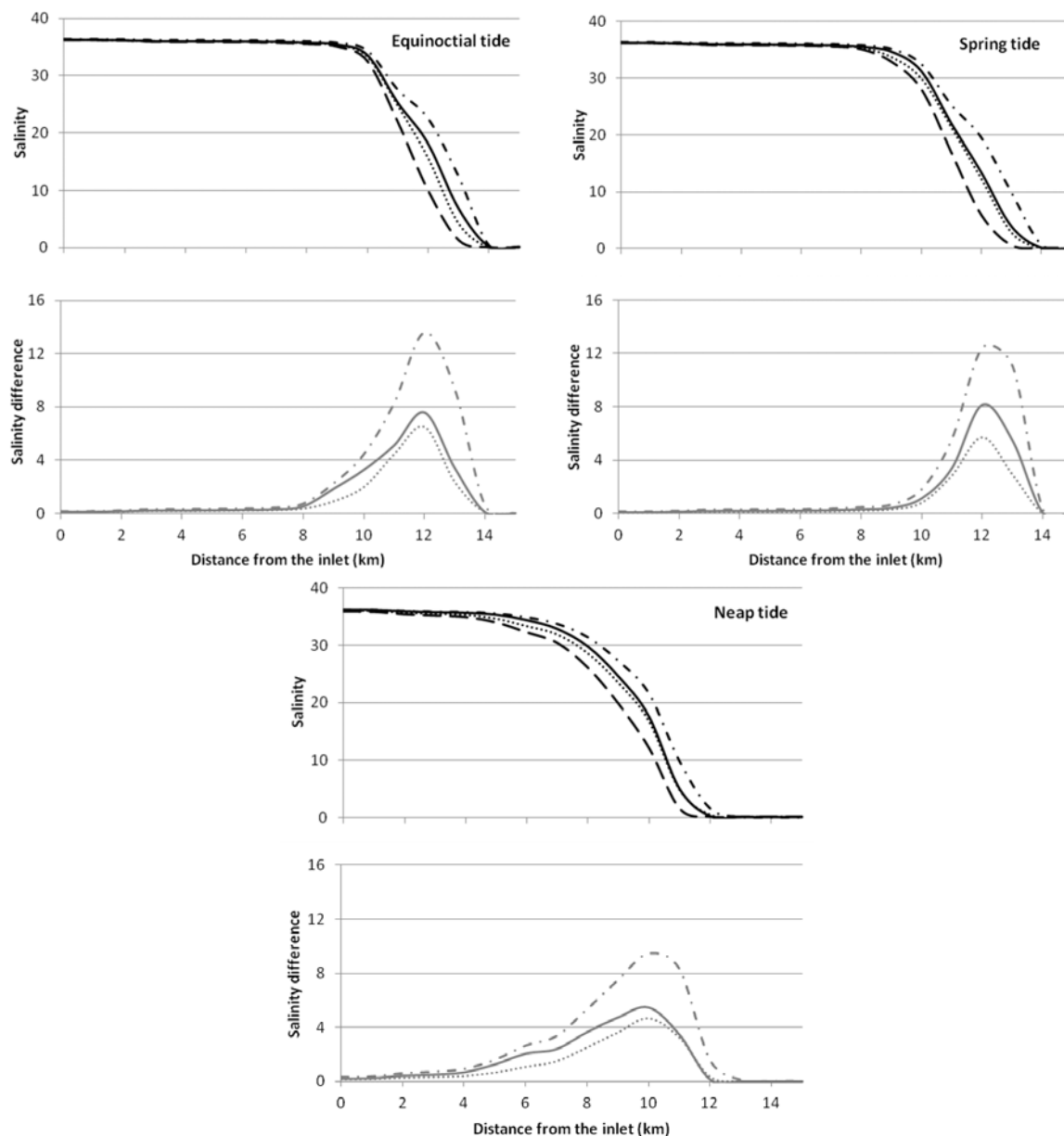
Figure 6.3 Maximum salinity along Espinheiro channel for each scenario and difference between Future and reference scenarios at wet season (black dashed line: A0 scenario; black solid line: A1 scenario; black dotted line: A2 scenario; black dashed-dotted line: A3 scenario; gray solid line: A1-A0 scenarios; gray dotted line: A2-A0 scenarios; gray dashed-dotted line: A3-A0 scenarios).

From Figure 6.4, referent to simulations in dry season, should be highlighted, once more, the null salinity gradient in the B2 and B3 projected scenarios, for which is considered a practically null river flow projection (Figure 4.4). Consequently, the maximum salinity differences along the channel present the same tendency when comparing B2 and B3 scenarios with the reference one. Moreover, the most notable difference for B2 and B3 scenarios relative to B0 scenario (maximum difference of 18 at channel's head for spring tide) has its bases in the fluvial flow occurrence in reference conditions as seen in Figure 4.4, despite its low significance. The B1-B0 differences (maximum difference of 3.5 once more at channel's head for spring tide) are exclusively due to sea level rise, as the river flow is maintained.
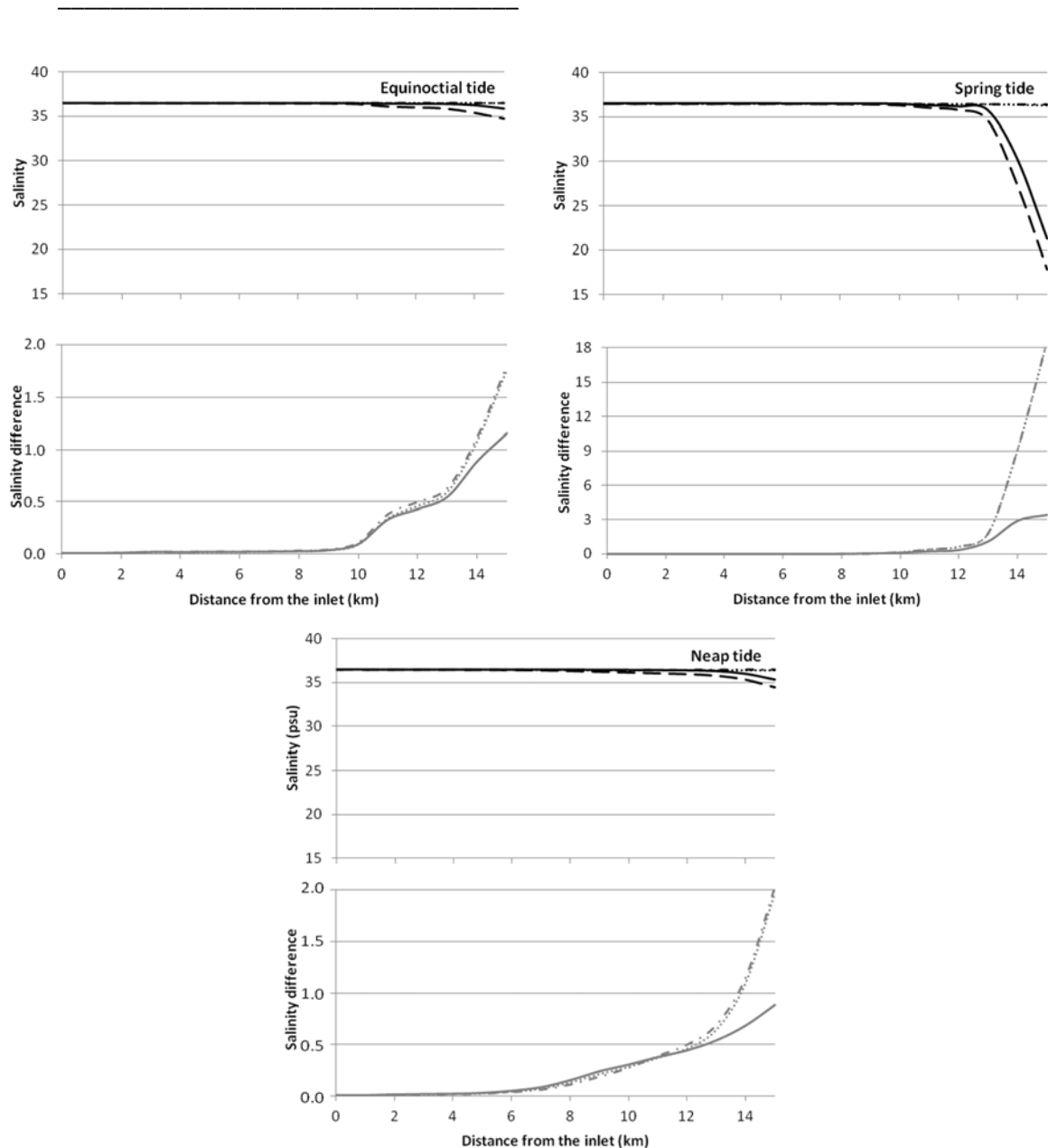
Figure 6.4 Maximum salinity along Espinheiro channel for each scenario and difference between future and reference scenarios at dry season (black dashed line: B0 scenario; black solid line: B1 scenario; black dotted line: B2 scenario; black dashed-dotted line: B3 scenario; gray solid line: B1-B0 scenarios; gray dotted line: B2-B0 scenarios; gray dashed-dotted line: B3-B0 scenarios).

In dry conditions, the already high salinity concentrations are intensified by sea level rise and river flow reduction, being this impact only visible in the channel's head. Indeed, while the salinity gradient remains its characteristics in wet conditions, from reference to future scenarios, in dry conditions this gradient tends to zero.

The Table 6.1 presents the average difference of maximum salinity in each channel, for all the conditions studied. Analyzing these results, the higher average differences for maximum salinity in wet season occurs at neap tide (4.30 for A3 – A0 difference at Ílhavo channel) and the lower at equinoctial tide (0.85 for A2 – A0 difference at Espinheiro channel). These average differences are very significant in this season for A3 scenario. Indeed, these differences correspond approximately to the sum of the A1 – A0 and A2 – A0 average differences, as A3

scenario computed results combines the effect of rising sea level (differentiation condition for A1 relative to A0 scenarios) and river flow reduction projected (differentiation condition for A2 relative to A0 scenarios).

In dry season, the average differences of maximum salinity between reference and future scenarios are not so clear, due to negligible river flow contributions (Figure 4.4). As a consequence, at dry conditions salinity gradient practically doesn't exist.

Table 6.1 Average difference of maximum salinity found between future and reference scenarios for each channel, at wet and dry seasons.

	Wet Season			Dry Season		
	A1-A0	A2-A0	A3-A0	B1-B0	B2-B0	B3-B0
Espinheiro Channel						
Equinoctial tide	1.26	0.85	2.14	0.23	0.28	0.30
Neap tide	1.57	1.17	2.67	0.24	0.33	0.34
Spring tide	1.45	1.10	2.58	0.52	1.93	1.94
S. Jacinto Channel						
Equinoctial tide	1.77	1.37	2.91	0.55	0.56	0.58
Neap tide	2.60	1.88	4.17	0.61	0.60	0.63
Spring tide	2.12	1.64	3.47	0.39	0.40	0.42
Ílhavo Channel						
Equinoctial tide	1.66	1.46	3.16	0.58	0.65	0.67
Neap tide	2.50	1.82	4.30	0.52	0.57	0.59
Spring tide	1.91	1.61	3.46	0.33	0.48	0.48
Mira Channel						
Equinoctial tide	0.82	1.38	2.23	0.52	0.74	0.78
Neap tide	1.37	1.46	2.95	0.67	0.98	0.97
Spring tide	0.86	1.42	2.28	0.32	0.63	0.63

6.2 Patterns adjustment

In order to analyze the spatial differences between reference and future scenarios, the maps depicting maximum salinity and maximum salinity differences were created, and are following described.

Figure 6.5 presents the maximum salinity fields for all the scenarios in wet season, obtained in the equinoctial conditions, as well as the differences field of A3 scenario relatively to reference scenario. At A0 scenario, higher salinity is confined to the lagoon central area and downstream limit of S. Jacinto, Ílhavo and Mira channels. From reference scenario to A1 projected scenario is observed an increase in salinity concentration in the lagoon central area and upstream S. Jacinto channel, as a consequence of MSL rise. In the A2 scenario, with the projected river flow decrease, salinity concentration increases mainly in the S. Jacinto channel. At A3 scenario the area with higher salinity expands to S. Jacinto channel's head and upstream regions of Mira and Ílhavo channels.
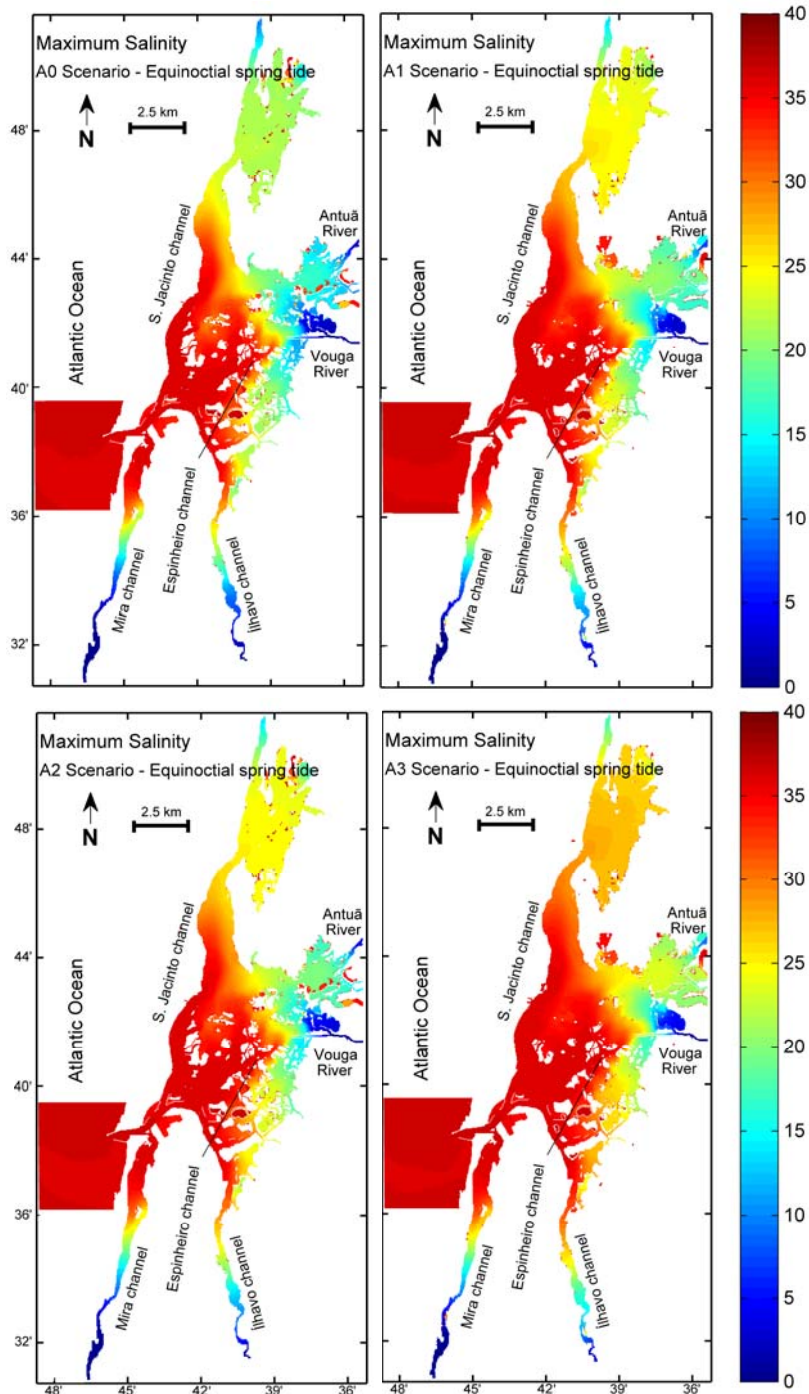
Figure 6.5 Maximum salinity fields for A0, A1, A2 and A3 scenarios at equinoctial tide.

Comparing scenario A3 (between the defined scenarios this is the more realistic and the one inducing higher adjustments) with A0 (Figure 6.6), the surrounding zone of the lagoon central area, the S. Jacinto channel's head, the Laranjo Basin and the middle zones of Mira and Ílhavo channels show larger increases in salinity, between 5 and 7.5. This projected salinity pattern adjustment denotes salinity intrusion in the upstream limits of Laranjo basin and lagoon central area, as well as of S. Jacinto channel.
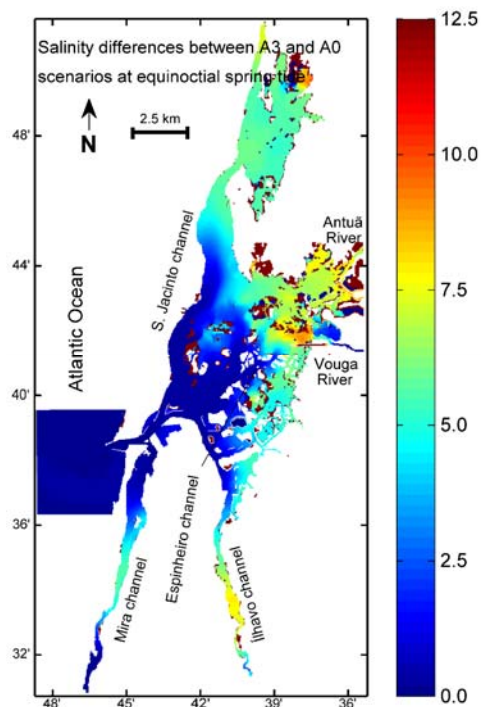
Figure 6.6 Salinity field difference between maximum salinity fields for A3 and A0 scenarios at equinoctial tide.

At neap tide the differences between future and reference scenarios under wet conditions are more significant than for larger tidal amplitudes (Figure 6.7). In the A0 scenario, salinity higher than 30 is confined to the lagoon's mouth, to the mouth of the S. Jacinto channel and to the Laranjo basin. The A3 scenario contrasts with the A0 in a large extension of the lagoon, with oceanic water expanding from the A0 to the A3 scenarios to almost all the lagoon central area, to the entire S. Jacinto channel, to the Laranjo basin and to the Ílhavo's channel initial stretch.

Figure 6.7 Maximum salinity fields for A0 and A3 scenarios at neap tide.

The difference between these two maximum salinity fields (Figure 6.8) reveals an extensive area with significant salinity increase: almost of the lagoon apart from the area near the mouth, the Laranjo basin upstream region and the Mira channel's head. This result is in accordance with the larger average differences found for neap tide and presented in Table 6.1.
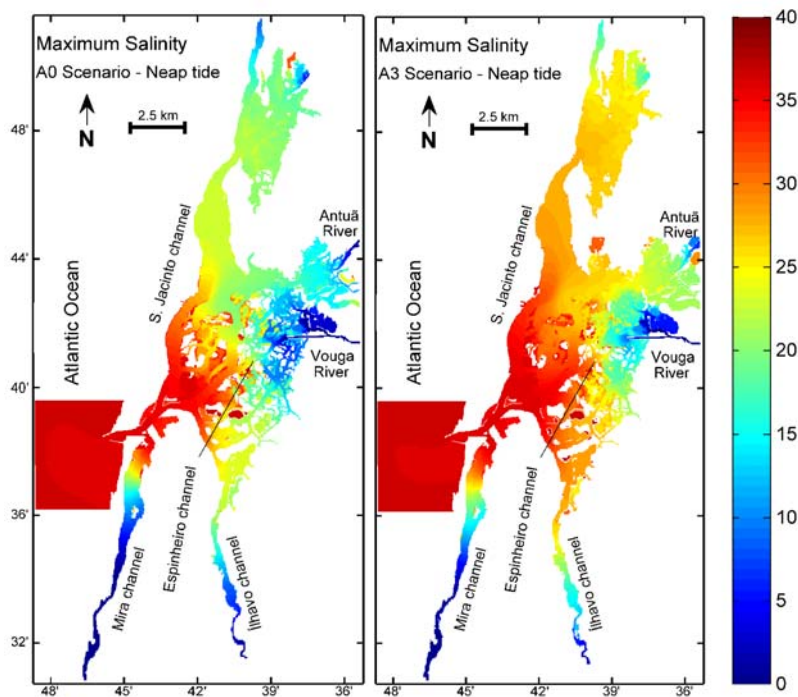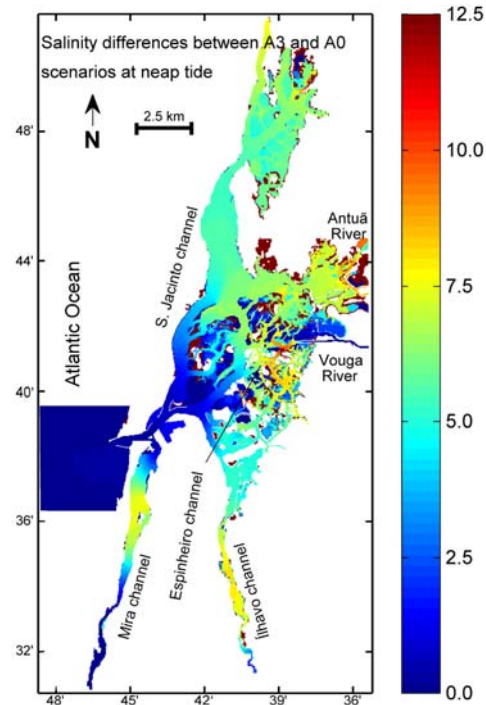

Figure 6.8 Salinity field difference between maximum salinity fields for A3 and A0 scenarios at neap tide.

In the dry season, the adjustments to projected forcing are less evident than in wet season. Indeed, considering the conditions which intensify salt intrusion (equinoctial tide), in the Future scenarios, due to the MSL rise and reduction of freshwater inflow, maximum salinities of 36.5 are found in the whole lagoon (Figure 6.9). Nevertheless, in the maximum salinity field for the reference scenario is possible to distinguish areas with lower salinity, near the main freshwater tributaries like channel's heads and upstream limit of Laranjo basin. For example, maximum salinity doesn't exceed 33 at Mira ditches head.

Based on the results presented in Figure 6.9, is expected that the actual limits of Ria de Aveiro lagoon will become entirely filled with sea water at high equinoctial tide in the B2 and the B3 scenarios (and also spring and neap tide, despite these results are not shown here), considering that flows tend to get null. In these conditions, at low tides this transitional water body will be also completely filled with sea water. At B2 scenario the same does not occur, as the freshwater inflow has more significance. In fact, a total annual average flow of 1.5 m^3/s for B0 scenario contrasts with 0.2 m^3/s for B2 scenario (see Tables 4.2 and 4.3, respectively). Combining MSL rise projected and river flow reduction (about 83% as projected, Table 4.3) the lagoon will be displaced landward, and saline intrusion is expected.
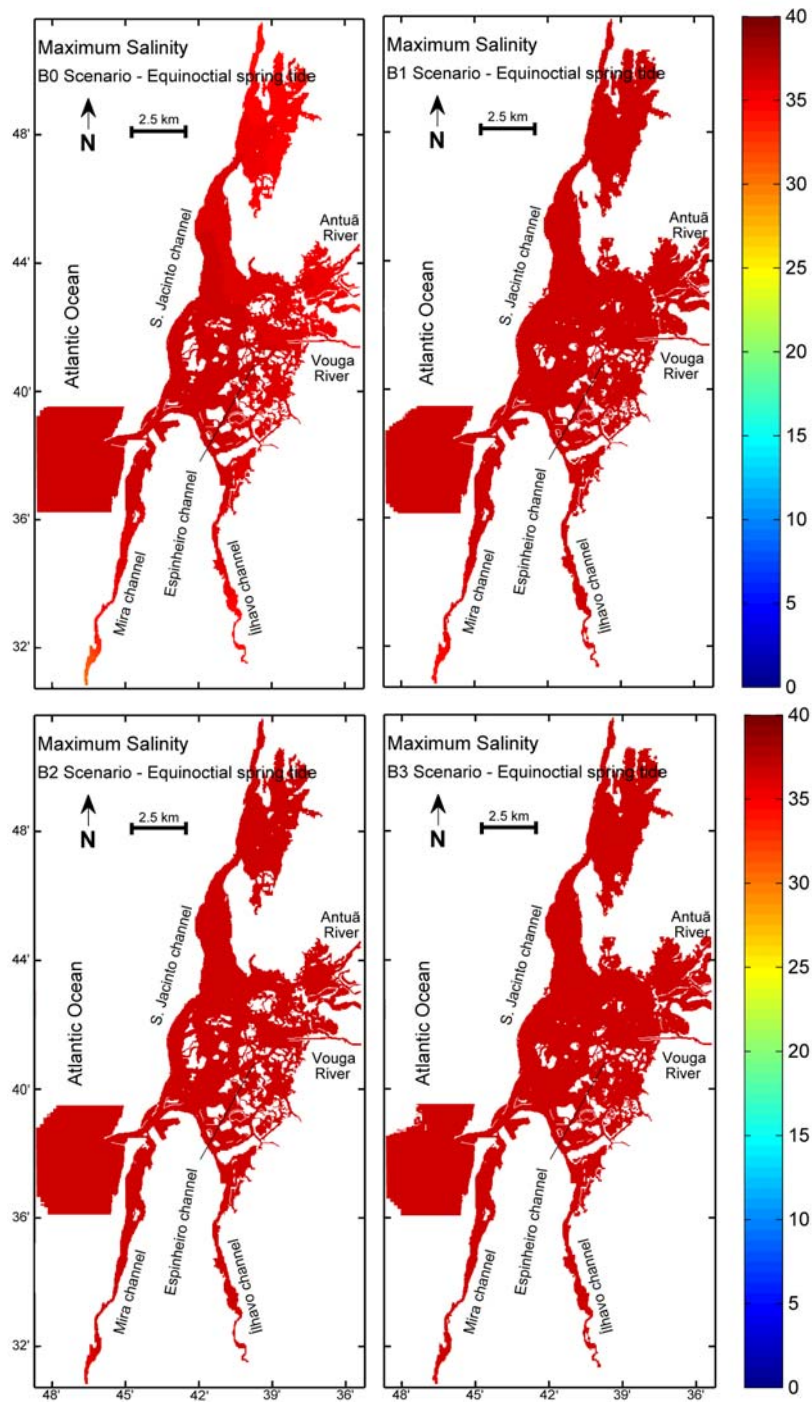
Figure 6.9 Maximum salinity fields for B0, B1, B2 and B3 scenarios at equinoctial tide.

The adjustment from reference conditions to B3 future scenario (Figure 6.10) does not exceed a salinity increase of 3.5 in the upstream areas.

Regarding maximum salinity field for A3 scenario in equinoctial tide (Figure 6.5), and the salinity patterns evolution from A0 scenario, it can be observed a tendency to an approximation between projected salt patterns in wet season to the reference salt patterns for dry season (Figure 6.9).
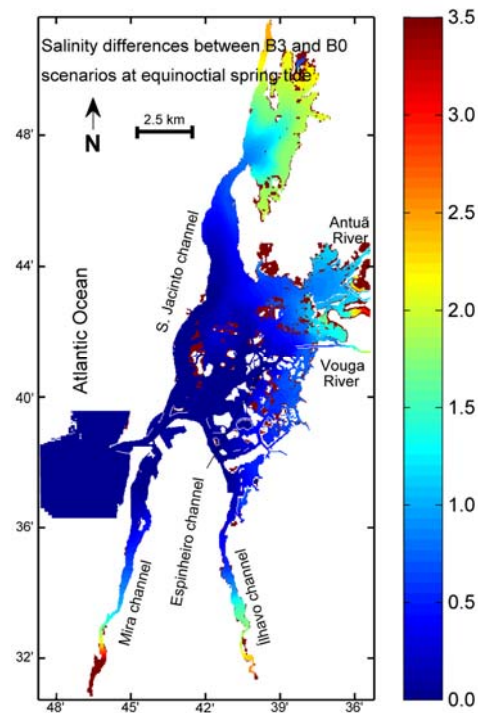
Figure 6.10 Salinity field difference between maximum salinity fields for B3 and B0 scenarios at equinoctial tide.

The higher increase in salinity, projected for the upstream regions of the lagoon at any of the future scenarios, is demonstrative of the saline intrusion effect. The salt intrusion will reach more upstream regions in dry seasons at equinoctial tide (Figures 6.9 and 6.10) as a consequence of the negligible flow projected (B3 scenario). During wet season, higher river flows will extend freshwater influence downstream the main channels in all scenarios. The salinity fields difference between the worst scenario A3 and A0 reference scenario (Figures 6.6 and 6.8) reveals a more significant salinity increase in the upstream northern and central zones of the lagoon (about 5 to 7.5) comparatively to the worst scenario in the dry season (a maximum increase of about 3.5).

6.3 Seasonal zonation adaptation according to Venice System

Once applied the Venice System zonation to the average salinity fields of the several scenarios under study, the zonations obtained from reference scenarios are compared with the ones achieved by Dias *et al.* (2011a), although those were obtained from measurements only conducted during tides of average amplitude. Zonations for both equinoctial and neap tide conditions at wet season (A0 scenario in Figures 6.11 and 6.12) reveal a landward displacement of all zones when compared with Winter zonations by Dias *et al.* (2011a). Particularly, in the modeled conditions (see Section 4.2 and mainly Figure 4.4), Euhaline and Polihaline zones (between 36.5 and 18) occupies almost all the lagoon central zone and the entire S. Jacinto channel, with Mesohaline, Oligohaline and Limnetic zones (salinity lower than 18) being restricted to Vouga channel's head, Laranjo basin, and Mira and Ílhavo channels. In Winter season, Dias *et al.* (2011a) identifies Euhaline and Polihaline zones confined to the inlet zone and lower estuary and to a small section of Mira channel. This discrepancy may be related with different river flow conditions and with model and measurement limitations. Zonation for dry season at equinoctial

tide and results obtained by Dias *et al.* (2011a) for Summer and Autumn seasons shows some similarity, with all the lagoon dominated by Euhaline conditions (salinity upper than 30) in the first case, and by Euhaline and Polihaline zones in Dias *et al.* (2011a) study.

Analyzing the zonations corresponding to the scenarios at wet season and equinoctial tidal conditions (Figure 6.11), is verifiable a landward displacement of each physical zone from reference scenario to the future scenarios, in tune with the salinity increase in the headwater channels direction (Figure 6.6).
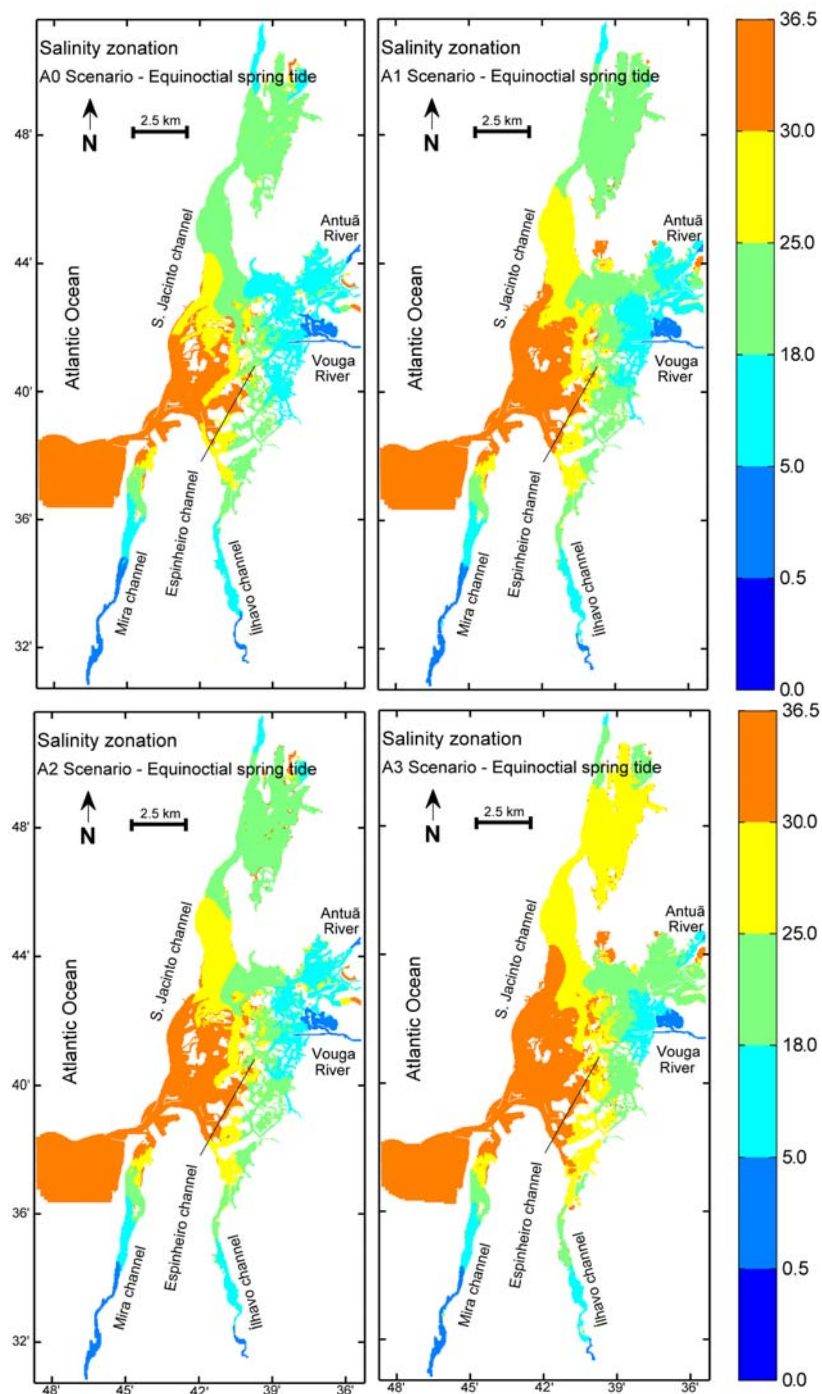

Figure 6.11 Zonations for A0, A1, A2 and A3 scenarios at equinoctial tide.

_____

MSL rise (A1 scenario) and projected river flow reduction (A2 scenario) induce quite similar zonation adjustments, as shown in Figure 6.12. Represented by gray colour are the areas where occurs upstream displacement of zones comparatively to A0 scenario. Indeed, from A0 scenario to A1 and A2 scenarios is verified an expansion of the Euhaline zone to more inland regions of the central lagoon area, the lower Polihaline zone (between 25 and 30) extends to the middle section of S. Jacinto channel, and a landward retreat of the Mesohaline zone occurs mainly in the Laranjo basin and in the Vouga channel's head. From A0 to A3 scenarios, the zonation adjustment is much more significant, as observable by the greater extension of gray area in Figure 6.12. The lower Polihaline zone expands to S. Jacinto channel's head and to more inland regions in the lagoon central zone, and middle Polihaline zone occupies the entire Laranjo basin. Mesohaline zone followed by Oligohaline zone stay confined to Laranjo basin and Vouga channel's head, and to the landward sections of Mira and Ílhavo channels.
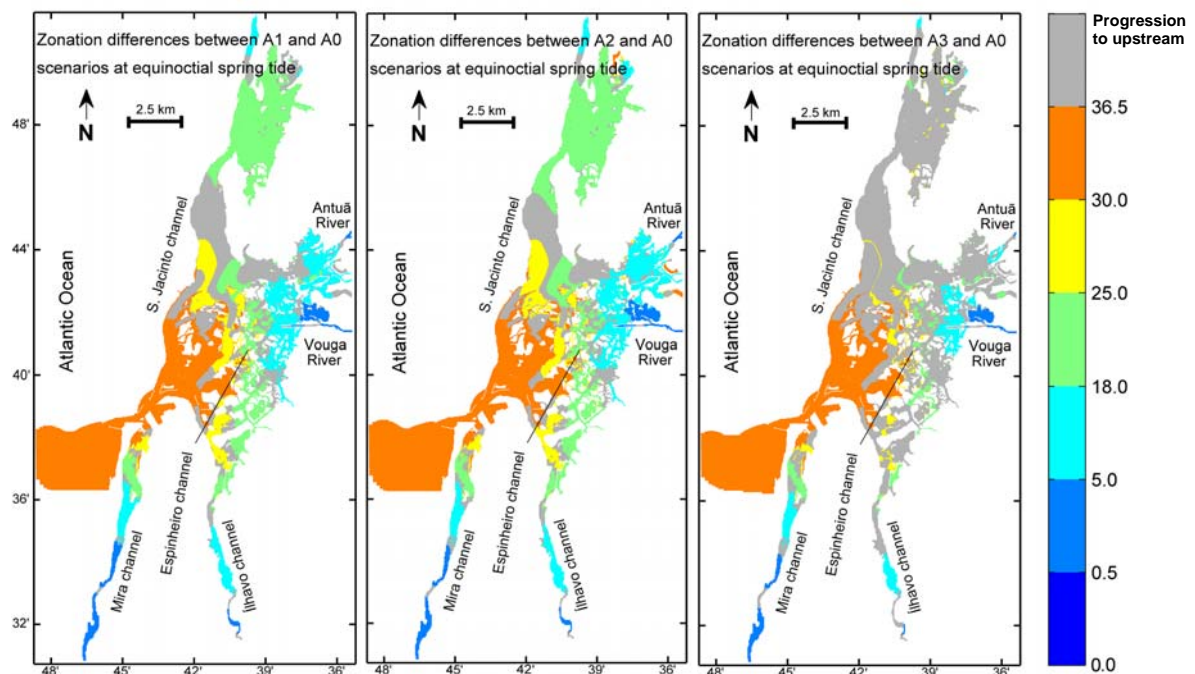
Figure 6.12 Zonation adjustment from A0 scenario to A1, A2 and A3 scenarios at equinoctial tide.

The most expressive zonation adjustment in wet conditions was obtained at neap tide with A3 scenario (Figure 6.13), well represented by widespread distribution of gray colour over the lagoon. The Euhaline zone expands from the lower estuary (A0 scenario) to the middle lagoon central zone. In A3 scenario lower Polihaline zone occupies the lagoon region classified as middle Polihaline zone at A0 scenario, and Mesohaline and Oligohaline zones stay, in general, confined to the channel's head.
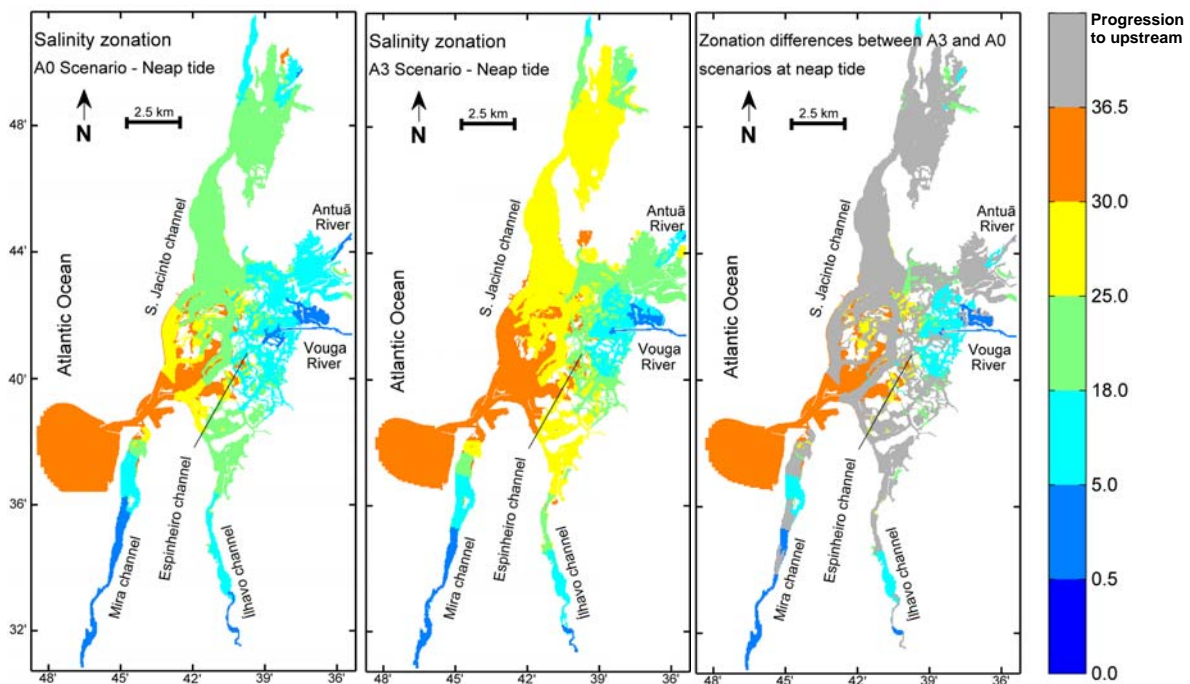
Figure 6.13 Zonations for A0 and A3 scenarios at neap tide and corresponding zonation adjustment.

In what concerns dry season scenarios, are just presented the reference scenario and B3 scenario in higher tidal amplitude conditions (conditions for which greater saline intrusion is expected), since no significant differences are observed in each zonation (Figure 6.14). In fact, due to the higher salinity concentrations all over the lagoon, about the entire lagoon domain is classified as Euhaline zone (saline concentration upper than 30) independently of the scenario considered. For reference scenario, at the upstream limit of Mira channel can be found a short section with lower Polihaline zone characteristics.
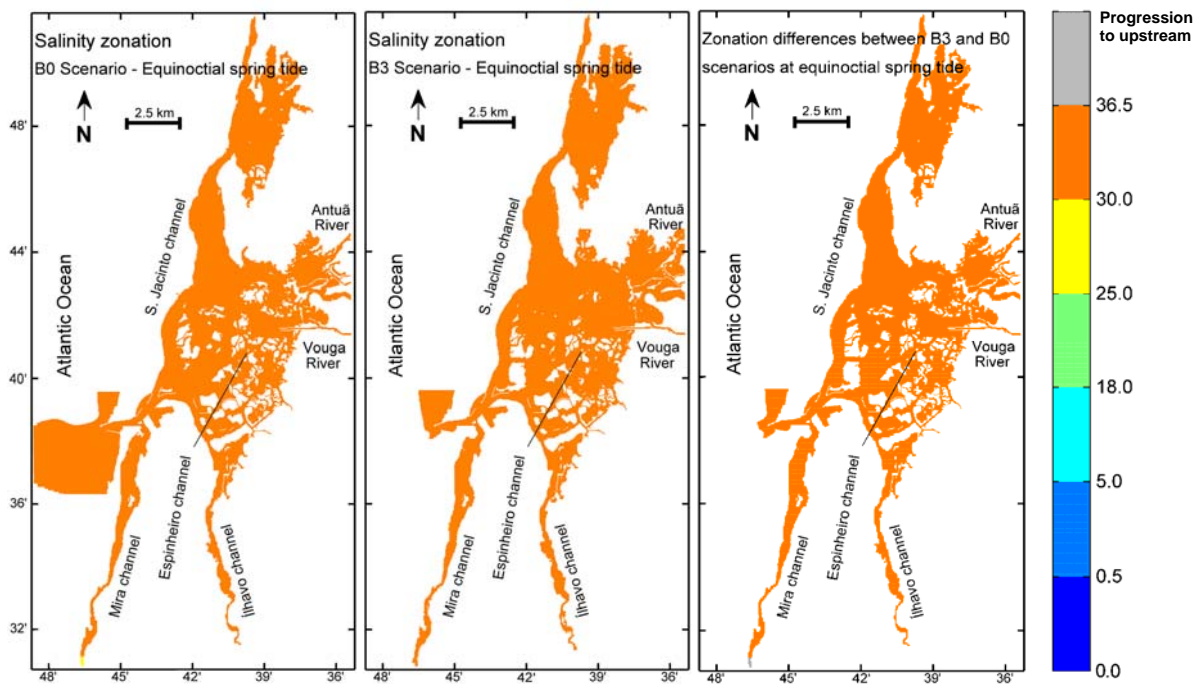
Figure 6.14 Zonations for B0 and B3 scenarios at equinoctial tide and corresponding zonation adjustment.

_____

Most of the studies of MSL rise effect in salinity distribution at estuarine environments identified in the literature (Grabemann *et al.*, 2001; Bhuiyan and Dutta, 2011; Chua *et al.*, 2011; Rice *et al.*, 2012; Hong and Shen, 2012) lead to the same findings of this study: the salt concentration will increase in estuarine environments and the brackish water will extend landward as MSL rises. The upstream saline increase as a consequence of a river flow projected reduction, most evident at A2 scenario (Figure 6.5), is in accordance with Beare and Heaney (2002), Robarts *et al.* (2005) and Chua *et al.* (2011) conclusions. The results of this study reveals that in future scenarios the salinity increase is larger in the upper lagoon regions in accordance with Rice *et al.* (2012) finding.

_____

7 Conclusions and recommendations for future work

This study has as main purpose to answer the question: How do seasonal saline distribution patterns are expected to adjust to climate change in Ria de Aveiro lagoon?

To answer to this question two objectives were formulated:

- Analyze the adjustment of the Ria de Aveiro water salinity patterns to changes in main forcing through numerical modeling; and
- Obtain new zonations of the Ria de Aveiro physical limits for the end of the XXI century, applying the Venice System to the projected modeled results.

To find answers to these objectives MOHID model was applied making use of an improved numerical bathymetry incorporating low laying lands until 10 meters relative to chart datum, reintroducing existing structures that limit water inland advance in conditions of higher water levels (dikes and walls), and actualizing with 2012 bathymetric data for the area under APA jurisdiction. The hydrodynamic and salt and heat transport models were successful calibrated, being able to reproduce with good accuracy the salt transport processes in the mouth and central area of the Ria de Aveiro.

Different future scenarios were defined for wet (A scenarios) and dry (B scenarios) conditions to study the impact of MSL rise and river flow regime changes, projected regionally for the end of the century according to A2 SRES scenario. These forcing where chosen due to be determinant in the establishment of salinity gradients in typical estuarine environments, as is the case of Ria de Aveiro lagoon. Results obtained to projected future conditions were confronted with simulations for reference conditions (zero scenarios) – local MSL and actual flow regime. Three future scenarios were defined: the 1st one considering local MSL rise; the 2nd one considering projected changes in flow regime in wet and dry seasons for the lagoon main tributaries; and the 3rd one taking into account MSL rise and changes in river flow regime projected. Simulation results were analyzed for different tidal conditions.

Salinity along channels

From the analysis of the maximum salinity changes along the lagoon main channels is observed an upstream displacement of the saline fronts generated in wet season for all the future scenarios relative to the reference ones (more pronounced for A3 scenario). The progression with A3 scenario is in the order of one to three km, depending on the channel and tide being considered. Note that saline fronts position variation due to the tidal amplitude variability is of greatest importance at any channel under study, comparatively to climate change effects. In dry conditions, the already high salinity concentrations increase even more in B3 scenario due to sea level rise and river flow reduction, being this impact only visible in the channels head. The results along the channels allowed concluding about the approximation of neap tide patterns at A3 scenario to the equinoctial tide patterns in A0 scenario.

In the Espinheiro channel, for A3 scenario, this upstream advection of the saline front is in the order of 1.5 km at equinoctial and spring tide, and of 1 km at neap tide. While in wet conditions the salinity gradient of the saline fronts remains approximately unchanged from reference to future scenarios (a value of about 8.0 km^{-1} in equinoctial conditions for all scenarios), in dry conditions this gradient tends to zero.

In wet season, the average differences of maximum channel-mean salinity for scenario A3 are higher than the obtained for dry season. These values range for wet season between 2.1 at Espinheiro channel (equinoctial tide) and 4.3 at Ílhavo channel (neap tide), and between 0.3 and 1.9 at Espinheiro channel (equinoctial and spring tides, respectively), for dry season.

Patterns adjustment

Analyzing the adjustments in maximum salinity concentration for the entire lagoon, the salinity increase is generalized over the lagoon but more expressive near the channels head for wet and dry conditions. In wet conditions, the maximum salinity may have an increase in the channels head of 5 to 7.5 assuming scenario A3 at equinoctial tide.

In dry conditions the salinity rise is not so pronounced in upstream regions, never exceeding 3.5 for B3 scenario at equinoctial tide. The higher increase in salinity concentration projected for the upstream regions of the lagoon, at any of the future scenarios, is demonstrative of the saline intrusion effect. At B2 and B3 scenarios, with negligible river flows, for high equinoctial tide the actual limits of Ria the Aveiro will become entirely filled with sea water, like occurring a lagoon displacement landward and consequent saline intrusion.

It can be observed a tendency to an approximation between projected salt patterns in wet season (scenario A3) to the reference salt patterns for dry season.

Seasonal zonation adaptation according to Venice System

The future seasonal zonations for wet season reveal a landward displacement of each physical zone, in tune with the salinity increase in the headwater channels direction. As expected, the zonation adjustment is much more significant from A0 to A3 scenarios than for the other two future scenarios. In equinoctial tide conditions the lower Polihaline zone expands to S. Jacinto channel's head and to more inland regions in the lagoon central zone, and middle Polihaline zone occupies the entire Laranjo basin. Mesohaline zone followed by Oligohaline zone stay confined to Laranjo basin and Vouga channel's head, and to the landward sections of Mira and Ílhavo channels. Summarily, in wet season all the physical zones defined in the Venice System can be identified and, under the influence of the projected conditions in study, tend to progress upstream.

No significant differences are observed in each zonation for dry conditions, being verified high salinity concentrations all over the lagoon duo to neglecting river inflows. For future scenarios the entire lagoon is classified as Euhaline zone (salinity upper than 30).

Briefly, in wet season projected scenarios the increase in saline concentration is more significant than for the dry season ones, being that increase more significant in the lagoon upstream regions. However, in dry season future scenarios the saline intrusion tends to go further inland due to negligible freshwater inflow (insignificant salinity gradient).

The results obtained, in particular: the salinity concentration increase and the salt inland intrusion; the upstream saline increase as consequence of river flow projected reduction; and the larger salinity increase in upper lagoon regions, are in accordance with the ones achieved in the majority of the studies related to MSL rise impact in estuaries salinity, found in literature (Chapter 2).

_____

In light of the achieved results and its coherence, the author considers that the objectives defined for this thesis were achieved with success and allow answering the main question formulated.

Despite the good results achieved, a more consistent study would have been obtained with source data for projections referent to the same period - relative MSL rise is referent to the period 2091-2100, while river flow was projected for 2071-2100.

Sea level rise and changes in river flow considered in this study result from the worst SRES scenario, the A2 scenario, enabling to simulate the highest potential impacts in terms of the lagoon salinity distribution. This methodological approach is based on the Precautionary Principle. Thereby, the obtained results intend to give a contribution to a long-term planning more able to prevent problems (Harremoës *et al.*, 2002).

Beyond the improvement of the procedure followed in this study, it would be of practical interest expand a similar analysis to other physical parameters determinant in water quality and lagoon's ecology, and to other lagoon environments. By this way, giving support to the development of strategies able to minimize impacts resulting from climate change in these environments. In what relates to future zonations obtained, it may be useful in ecological studies, namely for the Ria de Aveiro ecological vulnerability evaluation to climate change impacts.

References

Abbott, M.B. and Basco, D.R., 1994. *Computational Fluid Dynamics: An Introduction for Engineers*. Longman Scientific and Technical, London, 425 p.

Abecasis, C.K., 1961. *As Formações Lagunares e seus Problemas de Engenharia Litoral (contribuição para um estudo sistemático)*. Instituto Superior Técnico, Lisboa.

Alves, F.L., Silva, J.V., Pereira, C.A. and Sousa, L.P., 2011. Ten years assessment of ICZM Principles Applied at a Local Scale: Ria de Aveiro Case Study. *Journal of Coastal Research*, **64**, 1311-1315.

Anonymous, 1959. Symposium on the classification of brackish waters, Venice 8–14th April, *Archives Oceanography and Limnology*, **11(Suppl.)**, 1–248.

Antunes, C. and Taborda, R., 2009. Sea level at Cascais tide gauge: data, analysis and results. *Journal of Coastal Research*, **56(1)**, 218-222.

Arakawa, A. and Lamb, V., 1977. Computational design of the basic dynamical processes of the UCLA general circulation model. *Methods in Computational Physics*, **17**, 174-267.

Araújo, I.G.B., 2005. *Sea Level Variability: Examples from Atlantic Coast of Europe*. PhD Thesis, School of the National Oceanography Centre, Southampton, UK, 216 p.

Attrill, M.J. and Rundle, S.D., 2002. Ecotone or ecocline: ecological boundaries in estuaries. *Estuarine Coastal and Shelf Science*, **55**, 929-936.

Beare, S. and Heaney, A., 2002. Climate change and water resources in the Murray Darling Basin, Australia: impacts and adaptation. In: *Proceedings of 2002 World Congress of Environmental and Resource Economics*, California, 24-27 June, 33 p.

Bhuiyan, J.A.N. and Dutta, D., 2012. Assessing impacts of sea level rise on river salinity in the Gorai river network, Bangladesh. *Estuarine, Coastal and Shelf Science*, **96**, 219-227.

Boyer, T.P., Antonov, J.I., Baranova, O.K., Garcia, H.E., Johnson, D.R., Locarnini, R.A., Mishonov, A.V., O'Brien, T.D., Seidov, D., Smolyar, I.V. and Zweng, M.M., 2009. *World Ocean Database 2009. NOAA Atlas NESDIS 66*. S. Levitus (Ed.), U.S. Gov. Printing Office, Washington D.C., 216 p.

Burger, A.J., Hayden, B.P., Monaco, M.E., Nelson, D.M. and Mccormick-Ray, M.G., 1993. Biologically-Based Estuarine Salinity Zones Derived From a Multivariate Analysis. *Estuaries*, **16(2)**, 311-322.

Carriker, M.R., 1967. Ecology of estuarine benthic invertebrates: A perspective. In: Lauff, G.H. (Ed.), *Estuaries,* American Association for the Advancement of Science, **83**, 442-487.

CCSP, 2009. *Coastal Sensitivity to Sea-Level Rise: A Focus on the Mid-Atlantic Region. A Report by the U.S. Climate Change Science Program and the Subcommittee on Global Change Research*. Titus, J.G., Anderson, K.E., Cahoon, D.R., Gesch, D.B., Gill, S.K., Gutierrez, B.T., Thieler, E.R., Williams, S.J. (Ed.), U.S. Environmental Protection Agency, Washington D.C., USA, 320 p.

Cheng R.T., Burau J.R. and Gartner, J.W., 1991. Interfacing data analysis and numerical modelling for tidal hydrodynamic phenomena. In: Parker, B.B. (Ed.), *Tidal Hydrodynamics*, John Wiley & Sons, New York, USA, 201-219.

Cheng, R.T., Casulli, V. and Gartner, J.W., 1993. Tidal, residual, intertidal mudflat (TRIM) model and its applications to San Francisco Bay, California. *Estuarine, Coastal and Shelf Science*, **36**, 235-280.

Chippada, S., Dawson, C. and Wheeler, M., 1998. A Godonov-type finite volume method for the system of shallow water equations. *Comput. Methods Appl. Mech. Eng*, **151**, 105–130.

Chua, V.P., Fringer, O.B. and Monismith, S.G., 2011. Influence of Sea Level Rise on Salinity in San Francisco Bay. Unknown Journal. 46 p.

de Pascalis, F., Pérez-Ruzafa, A., Gilabert, J., Marcos, C. and Umgiesser, G., 2012. Climate change response of the Mar Menor coastal lagoon (Spain) using a hydrodynamic finite element model. *Estuarine, Coastal and Shelf Science*, **114**, 118-129.

Dias, J.A. and Taborda, R., 1988. Evolução recente do nível médio do mar em Portugal. *Anais do Instituto Hidrográfico*, **9**, 83–97.

Dias, J.M., 2001. *Contribution to the Study of the Ria de Aveiro Hydrodynamics*. PhD thesis, University of Aveiro, Portugal, 288 p.

Dias, J.M., Rodrigues, M., Leandro, S., Morgado, F., Oliveira, A. and Queiroga, H., 2011a. Caracterização Sinóptica dos Gradientes Ambientais na Ria de Aveiro. Parte I: Salinidade e Temperatura. In: Almeida, A., Alves, F.L., Bernardes, C., Dias, J.M., Gomes, N.C.M., Pereira, E., Queiroga, H., Serôdio, J., Vaz, N. (Ed.), *Atas das Jornadas da Ria de Aveiro 2011*, Universidade de Aveiro, CESAM – Centro de Estudos do Ambiente e do Mar, Aveiro, 141-150.

Dias, J.M. and Fernandes, E.H., 2006. Tidal and subtidal propagation in two atlantic estuaries: Patos lagoon (Brazil) and Ria de Aveiro lagoon (Portugal). *Journal of Coastal Research*, **SI(39)**, 1422-1426.

Dias J.M. and Lopes J.F., 2006. Implementation and assessment of hydrodynamic, salt and heat transport models: The case of Ria de Aveiro lagoon (Portugal). *Environmental Modelling & Software*, **21**, 1-15.

Dias, J.M., Lopes and J.F., Dekeyser, I., 1999. Hydrological characterisation of Ria de Aveiro, Portugal, in early Summer. *Oceanologica Acta*, **22**, 473-485.

Dias, J.M., Lopes, J.F. and Dekeyser, I., 2000. Tidal propagation in Ria de Aveiro Lagoon, Portugal. *Physics and Chemistry of the Earth (B)*, **25(4)**, 369-374.

Dias, J.M., Araújo, I.B. and Picado, A., 2011b. Dinâmica da maré na Ria de Aveiro. In: Almeida, A., Alves, F.L., Bernardes, C., Dias, J.M., Gomes, N.C.M., Pereira, E., Queiroga, H., Serôdio, J., Vaz, N. (Ed.), *Atas das Jornadas da Ria de Aveiro 2011*, Universidade de Aveiro, CESAM – Centro de Estudos do Ambiente e do Mar, Aveiro, 169-177.

Dias J.M., Sousa M., Bertin X., Fortunato A. and Oliveira A., 2009. Numerical modeling of the impact of the Ancão inlet relocation (Ria Formosa, Portugal). *Environmental Modelling & Software*, **24**, 711-725.

Dronkers, J.J., 1964. *Tidal Computations in Rivers and Coastal Waters*. North-Holland Publishing Company, 518 p.

Eisenreich, S.J., 2005. *Climate Change and the European Water Dimension. A Report to the European Water Directors (EU Report No. 21553).* European Commission- Joint Research Centre, 253 p.

Fairbridge, R.W., 1980. The estuary: its definition and geodynamic cycle. In: Olausson, E. and Cato, I. (Ed.), *Chemistry and Biogeochemistry of Estuaries*. John Wiley & Sons, New York, 1-35.

FitzGerald, D.M., Fenster, M.S., Argow, B.A. and Buynevich, I.V., 2008. Coastal impacts due to sea-level rise. *Annual Review of Earth and Planetary Sciences*, **36**, 601-647.

Frazão, O., Pereira, D., Santos, J.L., Dias, I., Dias, J.M., Vaz, N., Teixeira, M., Quintela, A., Ferreira, J., Ferreira, L.A. and Araújo, F.M., 2010. Industrialization of advanced optical technologies for environmental monitoring. *Clean Technologies and Environmental Policy*, **12**, 65-73.

Gibson, J.R. and Najjar, R.G., 2000. The response of Chesapeake Bay salinity to climate induced changes in streamflow. *Limnology and Oceanography*, **45**, 1764-1772.

Grabemann, H.J., Grabemann, I., Herbers, D. and Müller, A., 2001. Effects of a specific climate scenario on the hydrography and transport of conservative substances in the Weser estuary, Germany: a case study. *Climate Research*, **18**, 77-87.

Harremoës, P., Gee, D., MacGarvin, M., Stirling, A., Keys, J., Wynne, B. and Vaz, S.G., 2001. *Late lessons from early warnings: the precautionary principle 1896-2000*, Environmental issue report No 22, EEA, Copenhagen, 200 p.

Hilton, T.W., Najjar, R.G., Zhong, L. and Li, M., 2008. Is there a signal of sea-level rise in Chesapeake Bay salinity?. *Journal of Geophysical Research*, **113**, C09002.

Hong, B. and Shen, J., 2012. Responses of estuarine salinity and transport processes to potential future sea-level rise in the Chesapeake Bay. *Estuarine, Coastal and Shelf Science*, **104-105**, 33-45.

Hsu, M.H., Kuo, A.Y., Kuo, J.T., Liu and W.C., 1999. Procedure to calibrate and verify numerical models of estuarine hydrodynamics. *ASCE Journal of Hydraulic Engineering*, **125(2)**, 166-182.

Hull, C.H.J. and Tortoriello, R.C., 1979. *Sea-level Trend and Salinity in the Delaware Estuary*. Delaware River Basin Commission, 19 p.

Katsman, A.C., Hazeleger, W., Drijfhout, S.S., Oldenborgh, G.J. and Burges, G.J.H., 2007. *Climate Scenarios of SLR for the Northeast Atlantic Ocean: A Study Including the Effects of Ocean Dynamics and Gravity Changes Induced by Ice Melt*. Kluwer Academic Publishers, The Netherlands, 27 p.

Kjerfve B., 1986. Comparative oceanography of coastal lagoons. In: Wolfe, D.A. (Ed.), *Estuarine Variability*, Academic Press, New York, 63-81.

Leendertse, J., 1967. *Aspects of a Computational Model for Long Water Wave Propagation*. *Memorandum rh-5299-rr*, Rand Corporation, Santa Monica, 165 p.

Leendertse, J. and Liu, S., 1978. A three-dimensional turbulent energy model for non-homogeneous estuaries and coastal sea systems. In: Nihoul, J. (Ed.), *Hydrodynamics of estuaries and Fjords*, Elsevier, Amsterdam, 387-405.

Leitão, P.C., 2003. *Integração de Escalas e de Processos na Modelação do Ambiente Marinho*. PhD thesis, Instituto Superior Técnico. Universidade Técnica de Lisboa, Lisboa, Portugal, 296 p.

Leitão, P., Coelho, H., Santos, A. and Neves, R., 2005. Modelling the main features of the Algarve coastal circulation during July 2004: A downscaling approach. *Journal of Atmospheric and Ocean Science*, **10(4)**, 421-462.

Lopes, C.L., Silva, P.A., Dias, J.M., Rocha, A., Picado, A., Plecha, S. and Fortunato, A.B., 2011. Local sea lecel change scenarios for the end of the 21st sentury and potential physical impacts in the lower Ria de Aveiro (Portugal). *Continental Shelf Research*, **31**, 1515-1526.

Li, M., Zhong, L. and Boicourt, W.C., 2005. Simulations of Chesapeake Bay estuary: Sensitivity to turbulence mixing parameterizations and comparison with observations. *Journal of Geophysical Research*, **110**, C12004.

Martins, F., Leitão, P., Silva, A. and Neves, R., 2001. 3D modelling in the Sado estuary using a new generic vertical discretization approach. *Oceanologica Acta*, **24(1)**, 1-12.

Meehl, G.A., Stocker, T.F., Collins, W.D., Friedlingstein, P., Gaye, A.T., Gregory, J.M., Kitoh, A., Knutti, R., Murphy, J.M., Noda, A., Raper, S.C.B., Watterson, I.G., Weaver, A.J. and Zhao, Z.C., 2007. Global climate projections. In: Solomon, S., Qin, D., Manning, M., Marquis, M., Averyt, K., Tignor, M.M.B., Miller, H.L. Jr., Chen, Z. (Ed.), *Climate change 2007: the physical science basis. Contribution of working group 1 to the fourth assessment report of the intergovernmental panel on climate change*. Cambridge University Press, Cambridge, 747-845.

Mendes, R.P.S., 2010. *Modelação Numérica da Pluma Estuarina da Ria de Aveiro: Estudo Preliminar.* Mestrado em Meteorologia e Oceanografia Física, Departamento de Física, Universidade de Aveiro, Aveiro, 50 p.

Mendes, R., Vaz, N. and Dias, J.M., 2011. Numerical modeling changes induced by the low lying areas adjacent to Ria de Aveiro. *Journal of Coastal Research*, **64**, 1125-1129.

Miller, J.R. and Russell, G.L., 1992. The impact of global warming on river runoff. *Journal of Geophysical Research*, **97**, 2757-2764.

Moreira, M.H., Queiroga, H., Machado, M.M. and Cunha, M.R., 1993. Environmental gradients in a southern estuarine system: Ria de Aveiro, Portugal, implication for soft bottom macrofauna colonization. *Netherlands Journal of Aquatic Ecology*, **27(2-4)**, 465-482.

Müller, A., Grabemann, I. and Kunze, B., 1992. Water quality modelling: prediction of the transport of water constituents in the Weser estuary (Germany). In: Spaulding, M.L., Bedford, K., Blumberg, A., Cheng, R., Swanson, C. (Ed.), *Estuarine and coastal modeling*, American Society of Civil Engineers, New York, 405-417.

Najjar, R.G., Pyke, C.R., Adams, M.B., Breitburg, D., Hershner, C., Kemp, M., Howarth, R., Mulholland, M.R., Paolisso, M., Secor, D., Sellner, K., Wardrop, D. and Wood, R., 2010. Potential climate change impacts on the Chesapeake Bay. *Estuarine, Coastal and Shelf Science*, **86**, 1-20.

Nakićenović, N. and Swart, R., 2000. *Special Report on Emissions Scenarios: A special report of Working Group III of the Intergovernmental Panel on Climate Change*, Cambridge University Press, Cambridge, 570 p.

Neitsch, S.L., Arnold, J.G., Kiniry, J.R. and Williams, J.R., 2011. S*oil and Water Assessment Tool: Theoretical documentation, Version 2009. Texas Water Resources Institute Technical Report no. 406*, Texas A&M University System, Texas, 647 p.

Nicholls, R.J., 2010. Impacts of and responses to sea-level rise. In: Church, J.A., Woodworth, P.L., Aarup, T., Wilson, W.S. (Ed.), *Understanding sea-level rise and Variability*, Blackwell Publishing Ltd, Wiley, UK, 456 p.

Nicholls, R.J., Hoozemans, F.M.J. and Marchand, M., 1999. Increasing flood risk and wetland losses due to global sea-level rise: regional and global analyses. *Global Environmental Change*, **9(1)**, 69-87.

Nicholls, R.J., Wong, P.P., Burkett, V.R., Codignotto, J.O., Hay, J.E., McLean, R.F., Ragoonaden, S. and Woodroffe, C.D., 2007. Coastal systems and low-lying areas. In: M.L. Parry,M.L., Canziani,O.F., Palutikof,J.P., van der Linden, P.J., Hanson,C.E. (Ed.), *Climate Change 2007: Impacts, Adaptation and Vulnerability. Contribution of Working group II to the Fourth Assessment Report of*

_____

the Intergovernmental Panel on Climate Change, Cambridge University Press, Cambridge, UK, 315-356.

Pawlowicz, R., Beardsley, B. and Lentz, S., 2002. Classical tidal harmonic analysis including error estimates in MATLAB using T TIDE. *Computers and Geosciences*, **28**, 929-937.

Peltier, W.R., 2004. Global glacial isostasy and the surface of the ice-age earth: the ICE-5G (VM2) model and GRACE. *Annual Review of Earth and Planetary Science*, **32**, 111–149.

Picado, A., Dias, J.M. and Fortunato, A.B., 2010. Tidal changes in estuarine systems induced by local geomorphologic modifications. *Continental Shelf Research*, **30(17)**, 1854-1864.

Picado, A., Lopes, C.L. and Dias, J.M., 2011. Alterações hidrodinâmicas na Ria de Aveiro – Cenários futuros. In: Almeida, A., Alves, F.L., Bernardes, C., Dias, J.M., Gomes, N.C.M., Pereira, E., Queiroga, H., Serôdio, J., Vaz, N. (Ed.), *Atas das Jornadas da Ria de Aveiro 2011*, Universidade de Aveiro, CESAM – Centro de Estudos do Ambiente e do Mar, Aveiro, 115-122.

Rebelo, J.E. and Pombo, L., 2001. *Os peixes da Ria de Aveiro – Diversidade, Ecologia e Distribuição*. Aveiro, 111 p.

Rice, K.C., Hong, B. and Shen, J., 2012. Assessment of salinity intrusion in the James and Chickahominy Rivers as a result of simulated sea-level rise in Chesapeake Bay, East Coast, USA. *Journal of Environment Management*, **111**, 61-9.

Robarts, R., Kumagai, M. and Magadza, C.H., 2005. Climate change impacts on lakes: technical report of the session 'Ecosystem Approach to Water Monitoring and Management' organized at the World Water Forum II in Kyoto. *Climatic Change Ecosystem Approach to Water Monitoring and Management*, UNEP Publication, Nairobi.

Roeckner, E., Bäuml, G., Bonaventura, L., Brokopf, R., Esch, M., Giorgetta, M., Hagemann, S., Kirchner, I., Kornblueh, L., Manzini, E., Rhodin, A., Schlese, U., Schulzweida, U. and Tompkins, A., 2003. *The atmospheric general circulation model ECHAM5.* Part I: Model description. Max Planck Institute for Meteorology Rep. 349, 127 p.

Russell, G.L., Miller, J.R. and Rind, D., 1995. A coupled atmosphere-ocean model for transient climate change studies. *Atmosphere-Ocean*, **33**, 683–730.

Russell, G.L., Miller, J.R., Rind, D., Ruedy, R.A., Schmidt, G.A. and Sheth, S., 2000. Comparison of model and observed regional temperature changes during the past 40 years. *Journal of Geophysical Research*, **105**, 14891–14898.

Sánchez-Arcilla, A., González-Marco, D., Doorn, N. and Kortenhaus, A., 2008. Extreme values for coastal, estuarine, and riverine environments. *Journal of Hydraulic Research*, **46(2)**, 183-190.

Santos, A.J.P., 1995. *Modelo Hidrodinâmico Tridimensional de Circulação Oceânica e Estuarina*. PhD Thesis, Universidade Técnica de Lisboa, Lisboa, 273 p.

Smith, N.P., 1977. Metorological and tidal exchange between Corpus – Christi Bay, Texas, and the northwestern Gulf of Mexico. *Estuarine Coastal Marine Science*, **5**, 511-520.

Solomon, S., Qin, D., Manning, M., Chen, Z., Marquis, M., Averyt, K.B., Tignor, M. and Miller, H.L., 2007. *Climate Change 2007: The Physical Science Basis. Contribution of Working Group I to the Fourth Assessment Report of the Intergovernmental Panel on Climate Change*. Cambridge University Press, Cambridge, United Kingdom and New York, NY, USA, 996 p.

Teixeira, S., 1994. *Dinâmica Morfossedimentar da Ria de Aveiro (Portugal).* PhD Thesis, Faculdade de Ciências da Universidade de Lisboa, Portugal, 397 p.

Trancoso, A.R., Saraiva, Fernandes, L., Pina, P., Leitão, P. and Neves, R., 2005. Modelling macroalgae using a 3D hydrodynamic-ecological model in a shallow, temperate estuary. *Ecological Modelling*, **187**, 232-246.

Umgiesser, G. and Bergamasco, A., 1995. Outline of a primitive equation finite element model. In: *Rapporto e Studi*, vol. XII. Istituto Veneto di Scienze, Lettere ed Arti, Venice, Italy, 291-320.

Vaz, N., 2007. *Study of Heat and Salt Transport Processes in the Espinheiro Channel (Ria de Aveiro)*. Phd thesis, Universidade de Aveiro, Aveiro, Portugal, 151 p.

Vaz, N. and Dias, J.M., 2008. Hydrographic characterization of an estuarine tidal channel. *Journal of Marine Systems*, **70(1-2)**, 168-181.

Vaz N. and Dias J.M., 2011. Cross-sectional and stratification patterns induced by tidal and river discharge changes in a tidal channel: a modelling study. *Journal of Coastal Research*, **SI(64)**, 1614-1618.

Vaz, N., Dias, J.M. and Leitão, P.C., 2009. Three-dimensional modelling of a tidal channel: The Espinheiro Channel (Portugal). *Continental Shelf Research*, **29(1)**, 29-41.

Vaz, N., Dias, J.M., Leitão, P. and Martins, I., 2005. Horizontal patterns of water temperature and salinity in an estuarine tidal channel: Ria de Aveiro. *Ocean Dynamics*, **55**, 416-429.

Vaz, N., Dias, J.M., Leitão, P.C. and Nolasco, R., 2007a. Application of the Mohid-2D model to a mesotidal temperate coastal lagoon. *Computers and Geosciences*, **33(9)**, 1204-1209.

Vaz, N., Leitão P.C. and Dias J.M., 2007b. Channel-ocean exchange driven by tides and river flow: Espinheiro Channel (Portugal). *Journal of Coastal Research*, **SI(50)**, 1000-1004.

Vaz, N., Lencart e Silva, J.D. and Dias, J.M., 2012. Salt fluxes in a complex river mouth system of Portugal. *PLOS ON*, **7(10)**, e47349.

Vermeer, M. and Rahmstorf, S., 2009. Global sea level linked to global temperature. In: *Proceedings of the National Academy of Sciences of the Unated States of America*, 1-6.

von Storch, H., Schnur, R. and Zorita, E., 1998. *Szenarien und Beratung: Anwenderorientierte Szenarien für den norddeutschen Küstenbereich. Final report nº 01LK 9510/0*, Bundesministerium für Bildung und Forschung, Bonnf.

Walters, R.A., 1992. A three-dimensional, finite element model for coastal and estuarine circulation. *Continental Shelf Research*, **12**, 83-102.

Warner, J.C., Geyer, W.R. and Lerczak, J.A., 2005. Numerical modelling of an estuary: a comprehensive skill assessment. *Journal of Geophysical Research*, **110**, C05001.

Wilmott, C.J., 1981. On the validation of models. *Physical Geography*, **2**, 184-194.

Zhong, L., Li, M. and Foreman, M.G.G., 2008. Resonance and sea level variability in Chesapeake Bay. *Continental Shelf Research*, **28**, 2565–2573.